

Original Article

Cite this article: Peiro A and Simón JL (2022) The Río Grío–Pancrudo Fault Zone (central Iberian Chain, Spain): recent extensional activity revealed by drainage reversal. *Geological Magazine* 159: 21–36. <https://doi.org/10.1017/S0016756821000790>

Received: 7 January 2021
Revised: 7 July 2021
Accepted: 12 July 2021
First published online: 9 September 2021


Keywords:

Calatayud Basin; recent fault; active fault; tectonic geomorphology; planation surface; Plio–Quaternary; slip rate

Author for correspondence:

Alba Peiro, Email: apeiro@unizar.es

The Río Grío–Pancrudo Fault Zone (central Iberian Chain, Spain): recent extensional activity revealed by drainage reversal

Alba Peiro  and José L. Simón

Dpto Ciencias de la Tierra, Grupo Geotransfer-IUCA, Universidad de Zaragoza, Pedro Cerbuna 12, 50009 Zaragoza, Spain

Abstract

The NNW–SSE-trending extensional Río Grío–Pancrudo Fault Zone is a large-scale structure that obliquely cuts the Neogene NW–SE Calatayud Basin. Its negative inversion during the Neogene–Quaternary extension gave rise to structural and geomorphological rearrangement of the basin margin. Geological mapping has allowed two right-relayed fault segments to be distinguished, whose recent extensional activity has been mainly characterized using a deformed planation surface (Fundamental Erosion Surface (FES) 3; 3.5 Ma) as a geomorphic marker. Normal slip along the Río Grío–Lanzuela Fault Segment has induced hanging-wall tilting, subsequent drainage reversal at the Güeimil valley after the Pliocene–Pleistocene transition, as well as morphological scarps and surficial ruptures in Pleistocene materials. In this sector, an offset of FES3 indicates a total throw of *c.* 240 m, resulting in a slip rate of 0.07 mm a⁻¹, while retrodeformation of hanging-wall tilting affecting a younger piedmont surface allows the calculation of a minimum throw in the range of 140–220 m after the Pliocene–Pleistocene transition, with a minimum slip rate of 0.07–0.11 mm a⁻¹. For the late Pleistocene period, vertical displacement of *c.* 20 m of a sedimentary level dated to 66.6 ± 6.5 ka yields a slip rate approaching 0.30–0.36 mm a⁻¹. At the Cucalón–Pancrudo Fault Segment, the offset of FES3 allows the calculation of a maximum vertical slip of 300 m for the last 3.5 Ma, and hence a net slip rate close to 0.09 mm a⁻¹. Totalling *c.* 88 km in length, the Río Grío–Pancrudo Fault Zone could be the largest recent macrostructure in the Iberian Chain, probably active, with the corresponding undeniable seismogenic potential.

1. Introduction

Recent tectonics can be revealed not only by direct observation of ruptures at the surface, but also by its imprint on landforms. Morphotectonics provides valuable information about the mechanisms responsible for deformation of the topography, and can decipher their relationship with crust uplift and subsidence due to folding or faulting (e.g. Ollier, 1981; Keller, 1986; Burbank & Anderson, 2012). In this way, geomorphological analysis contributes to the identification and mapping of active or recent faults, and therefore to the recognition of seismic sources and evaluate seismic hazard.

Some landforms, either planar (planation surfaces) or linear (shorelines, river terraces) can be used as direct markers of deformation. Their geometrical reconstruction, on maps or profiles, allows the quantification of fault displacement or overall relief uplift, while their dating permits the calculation of deformation rates (Bonow *et al.* 2006; Wagner *et al.* 2011; Ezquerro *et al.* 2020). In other cases, the tectonic signature on the landscape is subtler, and only qualitative diagnosis of recent tectonic movements can be achieved; drainage anomalies mostly fall within this category of evidence (Leeder & Jackson, 1993; Jackson *et al.* 1996; Goldsworthy & Jackson, 2000). Drainage reversal is a geomorphic sign that has been associated with extensional faulting and tilting in regions such as the East African Rift Valley (Ollier, 1981, pp. 175–6), the Tasman Sea rifting (Haworth & Ollier, 1992) or the Megara Basin in Greece (Leeder *et al.* 1991). In the latter, the present-day, S-flowing drainage pattern resulted from recent reversal; the previous N-flowing drainage system has been evinced by drainage and palaeocurrent analysis (Bentham *et al.* 1991).

The gentle relief of the central-eastern Iberian Chain (NE Spain), where relict landforms of diverse ages have been well preserved, provides an excellent laboratory for studying the interaction between tectonic and geomorphologic processes. Recent tectonic activity and seismicity of this intraplate region has been traditionally considered as low to moderate. It has been driven by extension linked to rifting of the Valencia Trough (Vegas *et al.* 1979; Roca & Guimerà, 1992), combined with crustal doming (Simón, 1982, 1989; Scotti *et al.* 2014). Since late Miocene time, the prevailing extension direction has changed from WNW–ESE to WSW–ENE (Simón, 1989), the latter being active up to the present day (Herraiz *et al.* 2000).

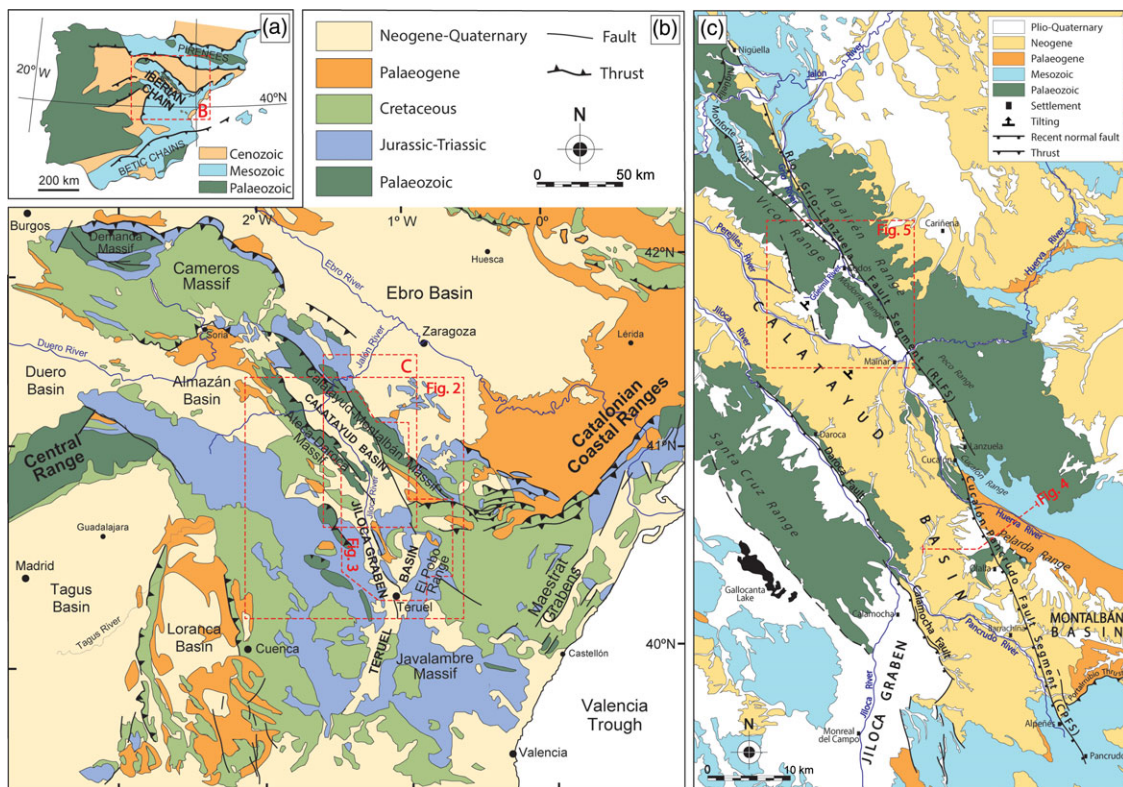


Fig. 1. (Colour online) (a) Location of the Iberian Chain within the Iberian Peninsula. (b) Geological sketch of the Iberian Chain, with location of the main Neogene–Quaternary extensional basins. (c) Geological map of the Río Grio–Pancrudo Fault Zone at the NE margin of the Neogene Calatayud Basin, with location of Figures 2–5.

Onshore extensional deformation has been accommodated by a number of large faults that bound grabens and half-grabens orthogonal to such extension directions: NNE–SSW (e.g. Teruel and Maestrat basins) and NNW–SSE (e.g. Jiloca Basin) (Fig. 1b). Recent (late Pliocene – Quaternary) activity of some of these faults (e.g. Concud, Sierra Palomera, Calamocha, Daroca, El Pobo, Peralejos, Teruel, La Hita and Valdecebro faults) has been characterized during the last decades from both structural and morphotectonic data. The contribution of late Neogene planation surfaces as widespread regional markers, allowing the calculation of fault throws and slip rates, has been decisive with this respect. These faults are modest in size, with lengths ranging from 5 to 19 km, maximum net displacements of 180–620 m and slip rates of 0.05–0.16 mm a⁻¹ for the last 3.8 Ma (Rubio & Simón, 2007; Lafuente *et al.* 2014; Simón *et al.* 2017, 2019; Ezquerro *et al.* 2020). Since late Miocene – Quaternary times, a tendency for the progressive concentration of crustal deformation on a smaller number of faults has been inferred, while those that remain active increase their slip rate (Simón *et al.* 2012; Ezquerro *et al.* 2020).

In parallel to such tectonic evolution and overall uplift, the region has undergone transition from endorheic to exorheic conditions, that is, from internal drainage paths, guided by the Neogene intramontane basins, towards external drainage guided by the large, peripheral fluvial systems (mostly Ebro, Tagus, Júcar and Turia rivers). Such transition was modulated by local interaction of rivers with faults and tilted blocks. Examples of river capture and river beheading of tectonic origin have been mostly described at the easternmost Iberian Chain, where the onset of a new drainage network oriented towards the Mediterranean Sea interacted with the development of the

conspicuous, NNE–SSW-trending Maestrat horst-and-graben system (Mateu, 1982; Pérez & Simón, 1993; Simón *et al.* 2013).

In this paper, we characterize a large recent extensional structure, very probably active, in a location further inland than those previously described in the Iberian Chain. It is here defined as the Río Grio–Pancrudo Fault Zone, comprising two segments separated by a narrow relay zone: Río Grio–Lanzuela (RLFS) and Cucalón–Pancrudo (CPFS). Its NNW–SSE-trending, 88-km-long trace cuts or bounds diverse geological domains (Calatayud–Montalbán Variscan folded block, Calatayud Cenozoic Basin, Alpine Utrillas Thrust), in which it has been locally identified using different names: Olalla Fault (Gabaldón *et al.* 1991), Alpeñés Fault (Tena & Casas, 1996), part of an interpreted Río Grio graben (Gutiérrez *et al.* 2013) or just the Río Grio Fault (Campos *et al.* 1996; Marcén, 2020). Its complex history since Variscan time, as well as the fragmented character of previous research, has prevented its identification as a single Neogene–Quaternary extensional structure (probably the largest within the Iberian Chain). Consequently, it has not received the attention that it merits as a potential first-order seismic source.

The purpose of this work is to shed some light on a series of ruptures, with diverse geological nature and history, that jointly define the Río Grio–Pancrudo Fault Zone. Because of the absence of widespread recent stratigraphic markers and the scarcity of outcrops where surface ruptures are exposed, the study of this large recent structure requires a geomorphological approach in addition to a purely structural approach. Our aims are to: (1) demonstrate Quaternary activity of the Río Grio–Pancrudo Fault Zone based on morphotectonic criteria, in particular using middle Pliocene – lower Pleistocene planation and pediment surfaces as deformation markers, and analyse two noteworthy cases of drainage reversal in

the framework of the regional transition from endorheism to exorheism; (2) achieve structural analysis of surficial ruptures along the RLFS (where the recent structure reactivates previous faults), discriminating between the kinematical imprint of contractive and extensional stages; and (3) infer fault throws and slip rates for distinct Plio-Quaternary time spans at the centre of the RLFS (Codos area) and in the CPFS (Cucalón–Olalla area).

2. Methods

The reconstruction of geomorphic markers and drainage anomalies are analysed using both geomorphological and sedimentological observations along the Río Grío–Pancrudo Fault Zone, while direct structural data at an outcrop scale allow us to characterize the geometry and kinematics of the RLFS. A detailed geological and geomorphological map has been constructed with the help of published maps at a 1:50 000 scale (Olivé *et al.* 1983), aerial photographs at a 1:30 000 scale, satellite orthoimages, digital elevation models (DEMs; pixel dimension 2 m) and the resulting hillshade images, and a field survey.

Palaeocurrent directions represent key data for demonstrating changes in fluvial patterns. The involved upper Pliocene and Pleistocene alluvial and fluvial sediments are mainly composed of gravel. In the absence of adequate three-dimensional (3D) exposures of sedimentary structures, such as channel bodies or cross-bedding, well defined sets of imbricated pebbles have allowed palaeocurrent directions to be interpreted at nine data sites. At each of these, 6–35 orientation data (average 16) of nearly plane pebble faces have been collected. The azimuth opposed to the average dip line of each imbricate pebble set has been taken as the local palaeocurrent direction.

Two good exposures of the damage zone at the trace of the RLFS have been surveyed. Data describing the orientation of rupture surfaces and associated kinematical indicators (slickenlines and small-scale drag folds) have been extracted from Palaeozoic materials of the footwall block. Two Pleistocene units affected by the fault zone at one of those localities have been dated by optically stimulated luminescence (OSL) in the Luminescence Dating Laboratory of Centro Nacional de Investigación de La Evolución Humana (CENIEH). Rose diagrams of palaeocurrents and stereoplots (equal-area, lower-hemisphere) of faults and slickenlines have been constructed using Stereonet 8 software (Allmendinger *et al.* 2012; Cardozo & Allmendinger, 2013).

In order to calculate vertical displacements of faults and infer net slip values, we have reconstructed the present-day geometry of Late Neogene planation surfaces and Plio-Pleistocene pediments offset by them. Maps of surface remnants were constructed using aerial photographs, topographic maps and DEMs, and the altitude of these remnants were interpolated for obtaining contour maps. The age of such morpho-sedimentary markers allows the calculation of fault slip rates. Further details on methodological problems concerning the use of planation surfaces as deformation markers are given in Section 4.a.

3. Geological setting

The Iberian Chain (Fig. 1a, b) is an intraplate, NW–SE-trending mountain chain located within the Iberian Plate, which developed during Cenozoic time under convergence with the European and African plates (Álvaro *et al.* 1979; Capote *et al.* 2002). It mainly resulted from inversion of several Mesozoic sedimentary basins, but also a thick succession of Palaeozoic units (up to 11 km;

Cortés-Gracia & Casas-Sainz, 1996) was re-folded in its central zone. In this sector, two elongated Palaeozoic-cored structural highs, the Calatayud–Montalbán and the Ateca–Daroca massifs, are separated by the NW–SE-trending Neogene Calatayud Basin (Fig. 1b, c).

The sinking of the Calatayud Basin (Fig. 1c) initiated under late stages of the Alpine compression during the Palaeogene–Neogene transition. The tectonic nature of the NE basin boundary is not well known because it is entirely covered by recent (Pliocene and Quaternary) alluvial deposits, but its SW boundary is an unequivocal contractive structure. At least in its central sector (Daroca area), Cambrian rocks overthrust lower Miocene continental deposits of the basin infill, while younger, middle–upper Miocene units lap onto the thrust front (Julivert, 1954; Colomer, unpub. thesis, University of Barcelona, 1987; Colomer & Santanach, 1988; Casas *et al.* 2017).

At the beginning of late Miocene time, the central-eastern Iberian Chain underwent an extensional tectonic period associated with rifting of the Valencia Trough (Vegas *et al.* 1979; Simón 1982; Roca & Guimerà 1992; Maillard & Mauffret, 1999; Fig. 1b). Onshore deformation is expressed by a large network of Neogene–Quaternary basins (Teruel, Jiloca, Munébrega, Maestrat), whose bounding faults mostly represent the negative inversion of previous compressional faults (Álvaro *et al.* 1979; Fig. 1b). The Calatayud Basin underwent reactivation of faults at its NE boundary (supposedly dipping towards the SW), downthrowing the Neogene infill. At the SW margin, the deeper part of the reverse Daroca fault was inverted during late Pliocene–Pleistocene time, giving rise to the Calamocha–Daroca extensional fault zone (Fig. 1c). The latter sinks the northern sector of the Jiloca graben and the Daroca half-graben with respect to the Neogene infill of the Calatayud Basin. Its throw has been estimated in the range of 210–250 m for the Calamocha rupture, by considering the offset of the uppermost, middle Pliocene lacustrine unit of the basin (Julivert, 1954; Colomer & Santanach, 1988; Gracia, 1992; Gutiérrez *et al.* 2008; Martín-Bello *et al.* 2014). The structure of the Calatayud Basin is similar to the neighbouring Daroca and Gallocanta half-grabens (Fig. 1c), with their respective faults at their NE margins. It all gives rise to a stepped profile of adjacent basins, with their infill tilted in the hanging-wall blocks of extensional faults.

During Neogene–Quaternary times, the regional stress field has evolved from (1) uniaxial extension with WNW–ESE-trending σ_3 trajectories during a first extensional episode (late Miocene – early Pliocene), to (2) nearly biaxial or radial extension (σ_1 vertical, $\sigma_2 \approx \sigma_3$) with σ_3 trending nearly WSW–ENE during a second episode (late Pliocene – Quaternary) (Simón, 1989; Arlegui *et al.* 2005; Liesa *et al.* 2019).

Under both compressional and extensional regimes, tectonic subsidence of the Calatayud Basin allowed the most complete Neogene series in the Iberian Chain to accumulate (Anadón *et al.* 2004). The sedimentary record consists of clastic alluvial sediments sourced at the basin margins, which grade towards central sectors into lacustrine–palustrine environments characterized by both evaporite and carbonate sedimentation (Gabaldón *et al.* 1991; Sanz-Rubio, 1999; Sanz-Rubio *et al.* 2003). Endorheic sedimentation culminates with a thin sequence of lower Pliocene palustrine carbonates (Páramo 2 unit) (Gabaldón *et al.* 1991; Anadón *et al.* 2004).

The geomorphological evolution of the central-eastern Iberian Chain includes several episodes of relief planation. The main episode has been classically referred to the so-called Fundamental

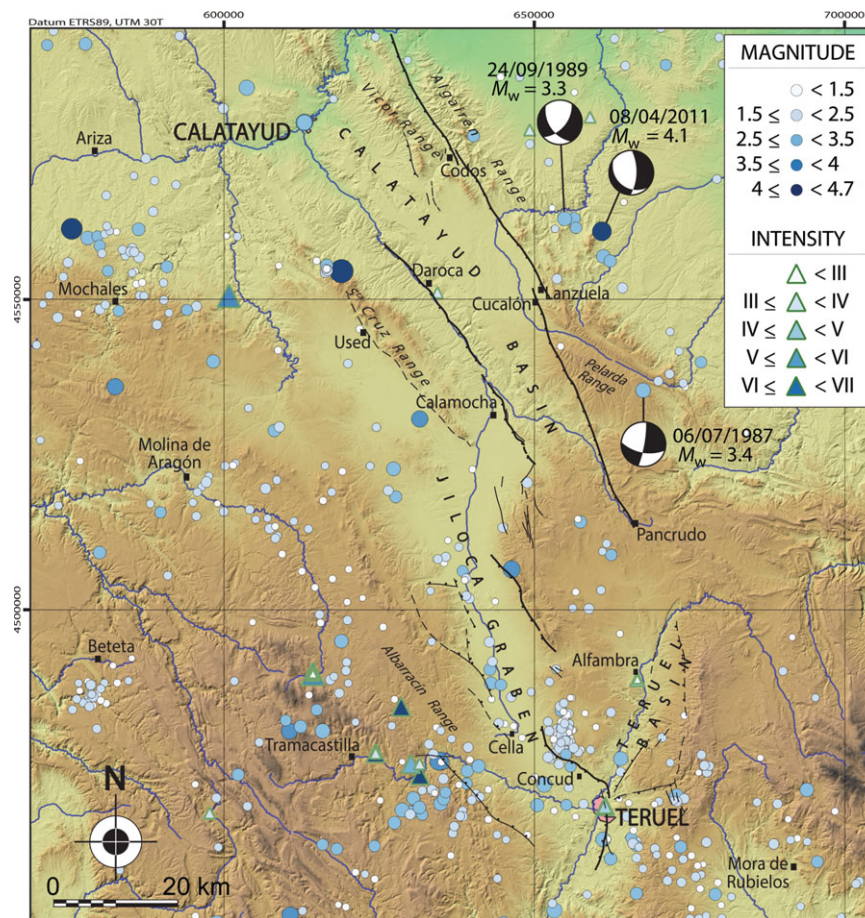


Fig. 2. (Colour online) Epicentre map of historic and instrumental earthquakes in the neighbourhood of the Calatayud Basin (<https://www.ign.es/web/ign/portal/sis-catalogo-terremotos>).

Erosion Surface (FES; Peña *et al.* 1984), and was traditionally correlated with the end of the endorheic filling of the Calatayud and Teruel basins (e.g. Simón, 1982). This surface has been recently divided into three sublevels, FES Upper Sublevel (FES1), FES *sensu stricto* (FES2) and FES Lower Sublevel (FES3), which in turn have allowed for finer physical correlation with sedimentary units, as well as more precise dating of planation episodes based on robust biostratigraphic and magnetostratigraphic data (Ezquerro, 2017; Simón-Porcar *et al.* 2019; Ezquerro *et al.* 2020). In this way, the age of FES3 is well constrained to the top of the M8 megasequence defined by Ezquerro (2017) (equivalent to the upper part of Páramo 2 unit; early Villafranchian in age; mammal biozone MN16; towards the base of chron C2An.3n; 3.5 Ma), while FES1 and FES2 merge into the top of M7 (lower part of Páramo 2 unit; late Ruscinian in age; MN15; middle part of C2Ar; 3.8 Ma) (Ezquerro *et al.* 2020). FES3 is overlaid by a Villafranchian (Pliocene–Pleistocene transition) alluvial system, comprising gravel and silt, that extends over most of the Neogene basins. The Villafranchian pediments of the Teruel area are dated to the earliest Pleistocene by macromammal fauna (Adrover, 1975; MN17 zone, 2.6–1.9 Ma) and, more accurately, by magnetostratigraphy (2.1–1.95 Ma; Sinusía *et al.* 2004).

The transition from endorheic to exorheic conditions in the study area is associated with the capture process of the Calatayud Basin. According to morphological and stratigraphical evidence, this is a diachronic process active since late Miocene time, which started with the capture of a primitive Jalón river

NW of the Algairén and Vicor Ranges (Gutiérrez *et al.* 1996, 2008, 2020; Fig. 1c). The Villafranchian pediments that spread towards the basin do not necessarily represent this rearrangement (Gutiérrez *et al.* 1996, 2008), since alluvial systems laterally grading into endorheic palustrine areas have been documented from early Pleistocene times, for example, in the Teruel area (Ezquerro *et al.* 2012), and have even persisted to the present in the Gallocanta depression (Gutiérrez *et al.* 1996) and the southern Jiloca Basin (El Cañizar lake; Rubio, 2004; Rubio & Simón, 2007). The Jiloca river, the main tributary of the Jalón river, captured the Jiloca graben during early Pleistocene time (Gutiérrez *et al.* 1996, 2008, 2020; Vacherat *et al.* 2018), becoming the longitudinal drainage of the Calatayud Basin, together with the primitive Perejiles and Grió rivers (Fig. 1c). During late Pleistocene time, part of the Calatayud Basin was also captured by the Huerva river (Gutiérrez *et al.* 2008). This progressive transition to exorheic conditions is overall controlled by the base-level drop of the Ebro river, although locally influenced by tectonic activity.

Historical and instrumental seismicity of the region is low to moderate (Fig. 2). Epicentres are concentrated close to the western margin of the Jiloca graben, in the relay zone between Conclud and Sierra Palomera faults, and in the western margin of the Calatayud Basin (<https://www.ign.es/web/ign/portal/sis-catalogo-terremotos>). No significant epicentre clustering occurs along the Río Grió–Pancrudo Fault Zone, the southern sector of the Calatayud Basin or the northern sector of the Jiloca graben (Fig. 1c). Before the instrumental period (maximum magnitude $M = 4.4$), intensities

up to VI–VII were recorded in the Albarracín range (1848) and IV–V in the Jiloca graben (1828). Focal depths typically range from 5 to 15 km, that is, within the brittle crust above the basal detachment level identified by Roca & Guimerà (1992). Most of the available focal mechanisms correspond to normal faults, and are consistent with the WSW–ENE- σ_3 -trending trajectories of the regional active stress field (Herraiz *et al.* 2000).

4. The Río Grío–Pancrudo Fault Zone: general structure and evidence of recent activity

4.a. Morphotectonic overview based on analysis of planation surfaces

Late Neogene planation surfaces have been recurrently used in the Iberian Chain for both identifying recent structures and assessing their vertical offsets and deformation rates (e.g. Peña *et al.* 1984; Gracia *et al.* 1988; Ezquerro *et al.* 2020). In our case, FES2 and FES3 surfaces and their coeval sedimentary levels provide potentially useful, mixed geomorphic–stratigraphic markers for this purpose, by allowing the construction of their corresponding structural contour maps.

Two main challenges have to be faced: constraining the age of each geomorphological marker, and ensuring its degree of flatness. The first issue has been adequately discussed and established in Section 3: FES2 and FES3 surfaces have been precisely dated to 3.8 and 3.5 Ma, respectively. The second issue should be justified, since continental planation surfaces can show gentle (short- to middle-wavelength) unevenness, or locally connect with residual, non-flattened reliefs through pediment slopes. Simón (1982, 1989) discussed this problem for the FES surface, recognizing that the amplitude of its unevenness meant that widely spaced contours (100 m) were required to represent its present-day geometry with adequate precision. At present, we realize that such an amplitude spans different sublevels that had not been recognized at that time; both the local difference in height between FES2 and FES3 and the local unevenness within each sublevel usually lies within the range 10–40 m. In consequence, we assume that: (1) vertical fault throws calculated from these sublevels implicitly include a maximum error bar of ± 40 m; and (2) a 50 m spaced contour map fits the precision of the actual roughness of FES2 and FES3 markers well, and can therefore be considered as reasonable for assessing recent movements (as previously proposed by Ezquerro *et al.* 2020). Such a level of uncertainty in the calculated fault throws results in errors for slip rates of *c.* 0.01 mm a⁻¹.

Such morphotectonic analysis should be primarily based on maps of planation surfaces covering large areas. In order to provide an overall morphotectonic view of the Río Grío–Pancrudo Fault Zone, we have synthesized several published maps in the Teruel region (Simón-Porcar *et al.* 2019; Ezquerro *et al.* 2020), as well as other maps constructed during our current research in the Jiloca and Calatayud basins. The result is shown in Figure 3, in which the (1) remains of several planation surfaces, (2) recent faults offsetting them and (3) contours of FES2 and FES3 depicting their present-day configuration jointly provide the best overall approach to describe the geometry of Plio-Quaternary deformation structures. FES2 contours have been drawn for the southern sector of the region, where the planation surface is better represented, while FES3 contours have been chosen for the northern sector. Despite such a difference, the systematic and continuous mapping over the entire region has ensured: (1) reliable identification of each erosion level, (2) age anchoring based on correlation

with sedimentary units in the Teruel Basin (see Section 3) and (c) an overview of the large-scale morphostructure.

4.b. Río Grío area

The northernmost RLFS crops out nearly parallel to the Grío river (Figs 1c, 3). It represents the negative inversion of the Variscan Nigiüella–Monforte Thrust, then reactivated as a transpressive structure during Palaeogene compression (Marcén & Román-Berdiel, 2015; Casas *et al.* 2016; Marcén, 2020), with occasionally coinciding rupture traces. Its recent extensional activity is revealed in different sectors of the Codos area, as extensively described in Section 5 and evidenced by: (1) tilting of the hanging wall deforming the FES3 and the Villafranchian pediment, (2) consequent post-Villafranchian drainage reversal and (3) local exposure of ruptures in Quaternary deposits.

4.c. Mainar–Lanzuela area

The prolongation of the RLFS to the SSE of the Grío river is clearly aligned with the NE margin of the Calatayud Basin, flanked by the Palaeozoic-cored Algairén and Peco Ranges (Figs 1c, 3). Both the Neogene series of the basin infill and FES3 are affected by a gentle, uniform tilting towards the structural highs. An extensional movement of the RLFS, similar to that registered at the Río Grío area, is inferred from this tilting. No outcrop of the fault trace has been found within this basin margin, partly because of the ensemble of Quaternary alluvial fans and pediments that overlies it. Nevertheless, the straight character of the contact between the lithological domains along the basin margin allows the fault trace to be identified. Near Lanzuela, an échelon, right-relay arrangement occurs between the RLFS and the CPFS. The spacing between these is 2 km, with an overlap of less than 2 km. The offset of the FES3 in this area allows a maximum vertical displacement of about 200 m to be inferred (Fig. 3).

4.d. Cucalón–Olalla area

South of Cucalón, the CPFS shows noticeable features of contractive deformation in the form of tight, hectometre-scale folds affecting the Palaeogene series of the Montalbán Basin (Figs 1c, 3). This series is abruptly interrupted by the fault, and a wide Quaternary alluvial fan that spreads from the fault zone towards the centre of the Calatayud Basin is indicative of recent activity.

Nevertheless, it is not easy to calculate precisely the amplitude and age of its vertical displacement because of uncertainties in the composition and morphostructure of both the footwall and the hanging-wall block in this sector. A key piece of evidence is a striking conglomerate unit, comprising rounded cobbles and boulders of Palaeozoic quartzite and Lower Triassic sandstone, which crops out at the highest part of this block (Pelarda Range summits, up to 1510 m in height; Fig. 1c). Its anomalous elevation and origin have been the objective of many conjectures, and the low quality of outcrops makes its characterization difficult. Maps published by the Spanish geological survey (IGME; Martín *et al.* 1977; Gabaldón *et al.* 1989a, 1991) indicate that it represents a nearly horizontal Plio-Quaternary unit that unconformably overlies the Palaeogene series; a thickness of *c.* 150 m could be inferred from those maps. In contrast, Moissenet (1980), Adrover *et al.* (1982) and Pailhé (1984) consider that it comprises a part of that folded Palaeogene series, then partially levelled by a late Neogene planation surface and uplifted by the extensional displacement of the

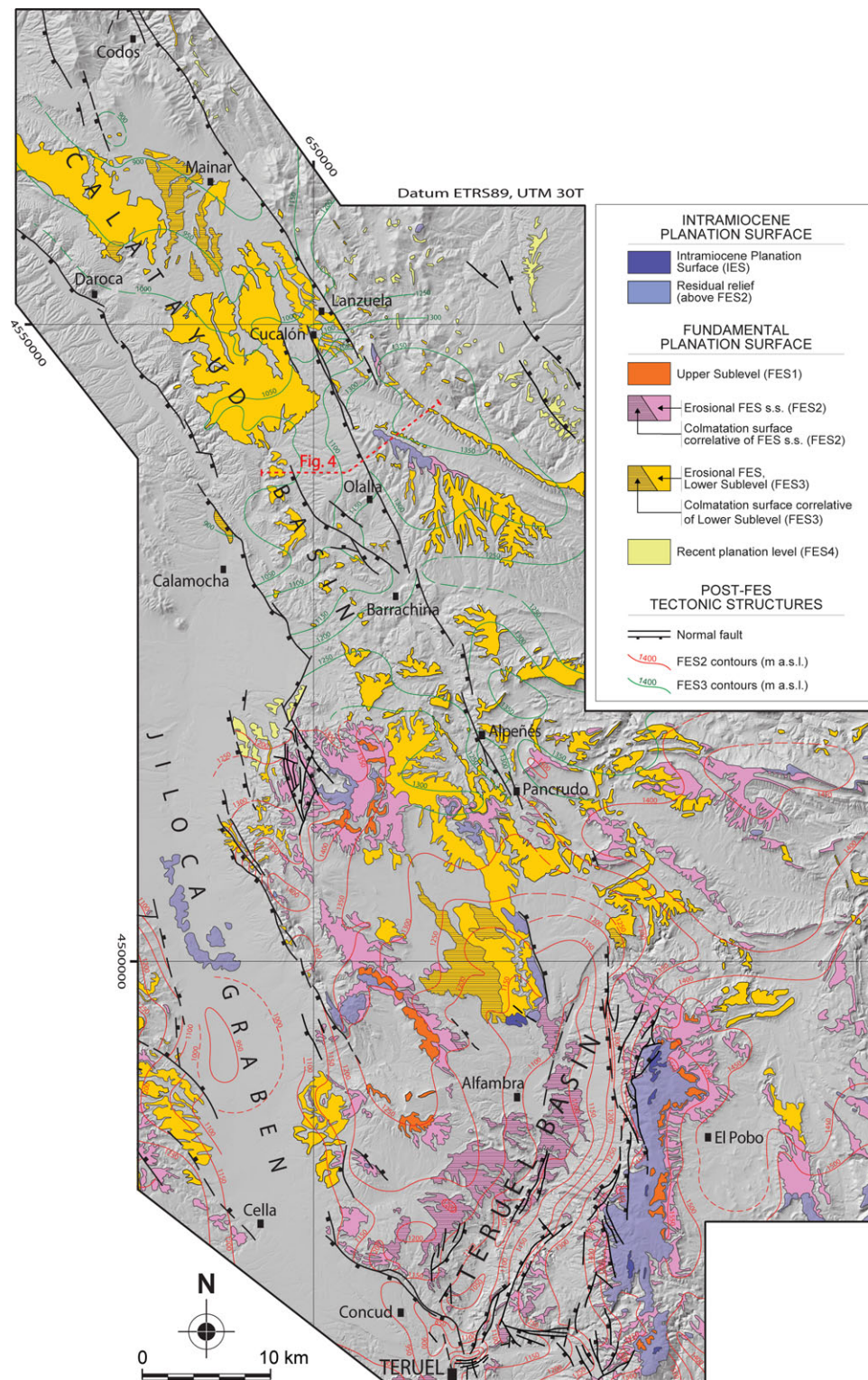


Fig. 3. (Colour online) Synthetic map of late Neogene planation surfaces in the surroundings of the Calatayud, Jiloca and Teruel basins, with location of Figure 4.

Cucalón–Olalla fault. The prominent Pelarda Range would represent a residual relief standing out above such a planation surface.

Recent and preliminary research conducted at the Pelarda Range revealed evidence in favour of the second interpretation (Fig. 4a, b). The quartzitic conglomerates probably correspond to the Oligocene Epoch (more specifically, to the upper part of unit

T3 defined by Pérez *et al.* 1983), since bedding planes and several occasional interbedded mud and sand layers above 1450 m above sea level (asl) are tilted similarly to the underlying Palaeogene series and show continuity with the latter. More recent deposits are limited to a thin (1–5 m) surficial cover mostly consisting of the same quartzitic cobbles and boulders reworked from the underlying Palaeogene strata. Such sedimentary cover is linked

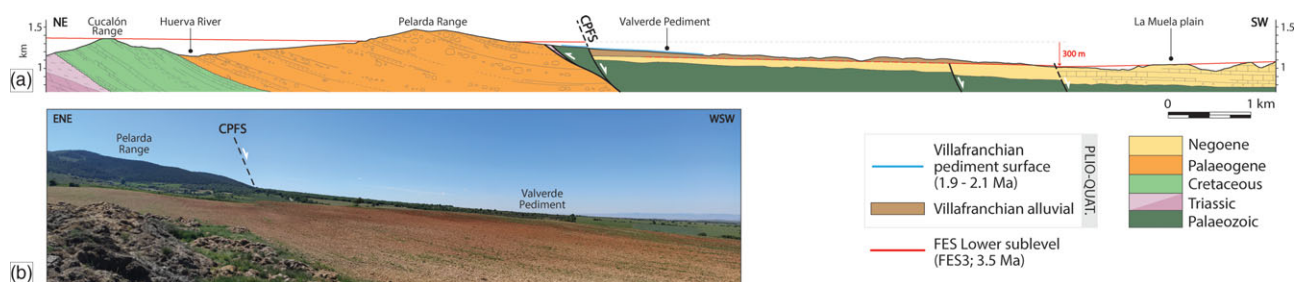


Fig. 4. (Colour online) (a) Cross-section through the Cucalón–Pancrudo Fault Segment (CPFS) at the Pelarda Range. Offset of the late Neogene planation surface (FES3) is indicated (see location in Figs 1c, 3). (b) Field view of the Pelarda Range mountain front.

to the FES3 planation surface, widely developed in the form of an extensive pediment (present-day mean slope *c.* 1.4°) lying between 1250 and 1390 m asl. Above this planation level, reduced remains of FES2 are preserved at 1400–1420 m, while the highest Pelarda summits, between 1420 and 1510 m, represent residual reliefs (Figs 3, 4a, b).

According to our present knowledge, the Neogene FES3 planation surface constitutes the only available deformation marker to obtain an overall estimate of post-3.5 Ma displacement on the fault zone. In the footwall block, at the western Pelarda Range transect (Figs 3, 4a), the remains of FES3 lie at 1320 m asl. In the hanging-wall block of the westernmost fault, FES3 is developed on Neogene materials of the Calatayud Basin, and to the NE of Daroca it correlates with the most recent lacustrine level capping the sedimentary sequence, analogue to that of the Teruel Basin (upper Páramo 2, Olivé *et al.* 1983; equivalent to M8 megasequence of Ezquerro, 2017; 3.5 Ma). Within this hanging-wall block, FES3 is downthrown to 1020–1030 m and is covered by red clastic deposits associated with a Villafranchian pediment. The overall fault zone has therefore undergone a total vertical offset of *c.* 300 m (the higher vertical offset recorded along the Río Grió–Pancrudo Fault Zone), partitioned among net slip on the faults depicted in Figure 4a and a gentle accommodation monocline. Assuming an approximate fault dip of 67° (which is similar to the average dip calculated for the RLFS, and lie within the 65–70° range of average dips for the main normal faults of the northern Teruel Basin; Ezquerro *et al.* 2020), its net slip for the last 3.5 Ma approaches 325 m, and its slip rate is *c.* 0.09 mm a⁻¹.

4.e. Barrachina area

The fault trace in this area is revealed by a succession of ruptures, not fully connected but markedly aligned. All of them cut and offset the Miocene and Pliocene carbonate units of the Calatayud Basin (Figs 1c, 3). Vertical offsets in the range of 50–120 m can be inferred for the FES3 surface.

4.f. Alpeñés–Pancrudo area

The CPFS shows visible contractive deformation (with a visible strike-slip component; Guimerà, 1988; Tena & Casas, 1996) in this area. It represents the limit where the Utrillas Thrust, in particular its western segment (Portalrubbio Thrust) is interrupted (Figs 1c, 3). Its recent extensional activation is not so evident. Once again, deformation registered by the FES3 has allowed a maximum vertical offset of about 100 m to be determined in this sector.

5. Detailed study at the Codos area

5.a. Morphostructure

The Codos area is located at the boundary between the central sector of the Calatayud Basin and the Calatayud–Montalbán massif (Figs 1c, 5). Crustal-scale thrusts and strike-slip faults inherited from Variscan and late Variscan tectonic periods, roughly parallel to the structural grain (NW–SE), are recognized within it (Cortés-Gracia & Casas-Sainz, 1996; de Vicente *et al.* 2009). The main Variscan structure is the Nigiüella–Monforte Thrust (Figs 1c, 5; Casas *et al.* 2016), formerly referred as Datos Thrust (Calvín-Ballester & Casas, 2014). The RLFS probably originated as a strike-slip fault during late Variscan stages, and obliquely cuts the Nigiüella–Monforte Thrust (Figs 1c, 5). Both structures partially share the rupture trace, but are distinguishable because the latter: (1) trends closer to NNW–SSE, (2) has a more pronounced dip and (3) shows noticeably thick fault rock bodies, especially at its northern sector (Casas *et al.* 2016). During the Palaeogene Period, the RLFS was reactivated as a dextral transpressive structure under the Alpine compression (variably oriented between N–S and NE–SW), giving rise to a complex internal structure made of anastomosing lenses of Ordovician and Triassic rocks exhibiting tight folds, pervasive foliation, fault breccia and fault gouge (Marcén & Román-Berdiel, 2015; Marcén, 2020).

The imprint of the Neogene negative inversion of the RLFS is much less noticeable than that of the contractive structure. The only macrostructural deformation feature extensively recognizable in geologic materials is gentle tilting of the Calatayud Basin Neogene infill towards the NE (Moissenet, 1980), particularly visible in the uppermost lacustrine carbonates (Páramo 1 and Páramo 2 units, early Pliocene in age; Olivé *et al.* 1983; Fig. 1c). Such tilting apparently represents roll-over accommodation of the hanging-wall block of the RLFS and Espigar fault, which jointly make the northeastern boundary of the Calatayud Basin in this sector (Figs 1c, 5).

As stated above, further evidence of recent fault activity can be expected from landforms. The bottom of the Calatayud Basin shows extensive remains of FES3 either topping the Páramo 2 carbonates or subtly cutting underlying Pliocene units (Figs 3, 5). Along the southern part of the study area, its altitude diminishes E-wards from about 950 up to 890 m asl, affected by the same tilting (*c.* 0.3°) already described for the Neogene units. The Villafranchian alluvial system is here associated with a wide embayment in the Espigar mountain front, NW of Langa del Castillo village (Campillo Plain, Fig. 5). Finally, both FES3 and the Villafranchian alluvium are incised by the drainage network tributary of the Perejiles river.

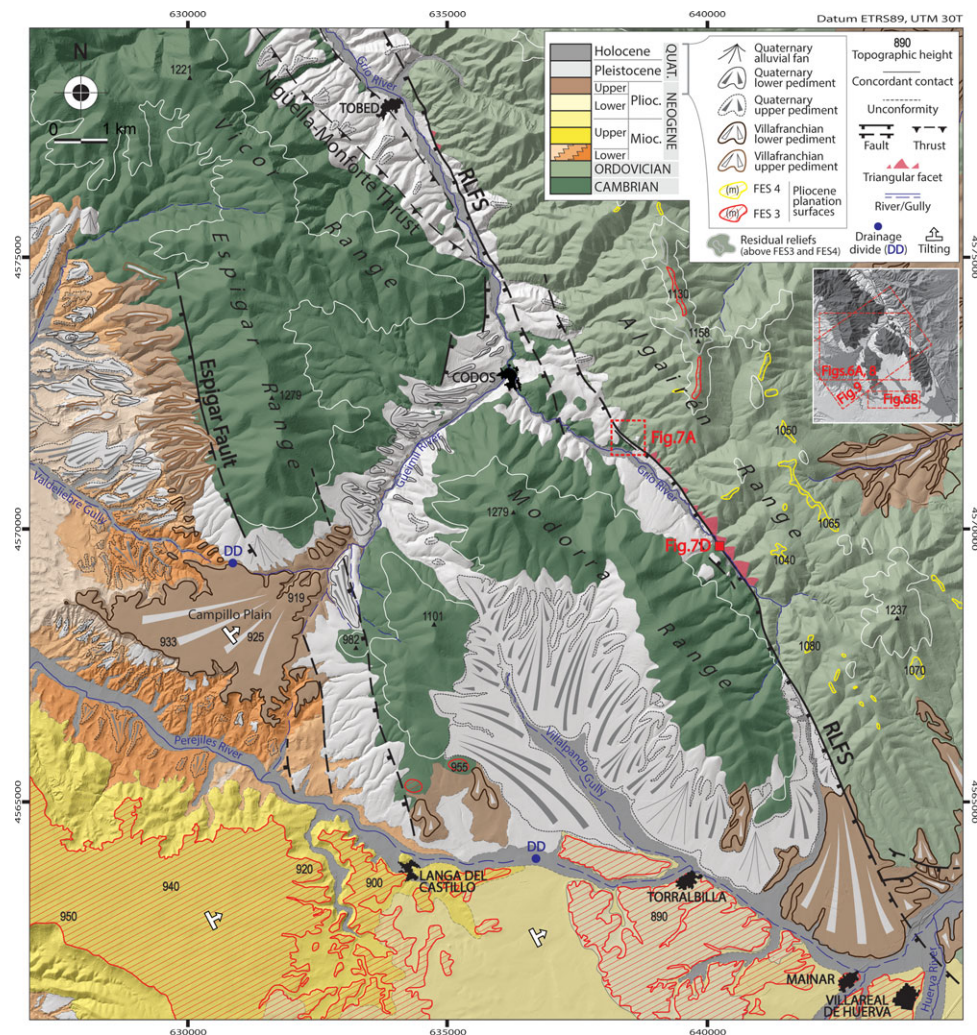


Fig. 5. (Colour online) Geological and morphostructural map of the Codos area affected by the Río Grio–Lanzuela Fault Segment (RLFS), in the NE margin of the Calatayud Basin (see location in Fig. 1c). Red squares and inset: location of Figures 6a, b, 7a, d, 8, 9.

FES3 has also been identified on the Palaeozoic massif (Algairén Range) at an altitude of 1130 m (Fig. 5). In this range, present-day heights of summits of the residual reliefs not levelled by this planation surface range from 1158 to 1237 m, and a new, more recent planation level (FES4) lies at 1040–1080 m asl (Fig. 5). Careful mapping and topographic correlation from the southern sector of the Calatayud Basin and neighbouring massifs have allowed the same FES3 planation surface to be determined in both the massif and the basin (Figs 3, 5). A post-FES3 vertical offset of about 240 m should therefore be interpreted for the RLFS in this area.

5.b. Evidence of drainage reversal

The northern sector of the Calatayud Basin and neighbouring ranges are drained by three main rivers (Jiloca, Perejiles and Grio) that flow towards the NNW, paralleling the Iberian structures. They join the transverse Jalón river, belonging to the Ebro drainage basin (Fig. 1b). To the south, the Huerva river also cross-cuts the eastern margin of the Calatayud Basin (Fig. 1c).

In the vicinity of Codos village, the Grio river is joined by a short, NE-flowing drainage, the Güeimil river, which exhibits a conspicuous drainage anomaly that reveals tilting of the overall Palaeozoic Vicor and Espigar ranges (Fig. 3). Today, the Güeimil

river flows towards the NE, into the Grio river. Nevertheless, the relief setting strongly suggests that the present-day Güeimil valley represents the same drainage corridor that fed the Villafranchian alluvial system of the Campillo embayment, sourced from the northeastern basin margin (Fig. 5). This would require that (1) the drainage during late Pliocene time was directed towards the SW, and (2) the Villafranchian pediment had the same slope sense, despite the present-day opposite slope of 0.5° towards the NE that should be attributed to the same tilting process undergone by the FES3 surface at the Calatayud Basin.

Such hypothesized drainage reversal should be tested from sedimentological observation. While the Villafranchian alluvial system is set at the Campillo Plain, Pleistocene fluvial and alluvial gravel fills the entire Güeimil and Grio valleys. These Pleistocene deposits show increasing thickness downstream along the Güeimil valley from a minimum of 5 m at the headwaters up to 80 m near Codos. A maximum thickness of 90 m has been reported by Gutiérrez *et al.* (2013) in the Tobed sector (Fig. 5). Both sedimentary units have been surveyed with the purpose of interpreting their respective palaeocurrent patterns. In nine outcrops, consistent orientations of imbricate pebbles have allowed such interpretation. The results (Fig. 6a) show (1) palaeocurrents towards the SW, W and NW in Villafranchian gravel, compatible with an alluvial

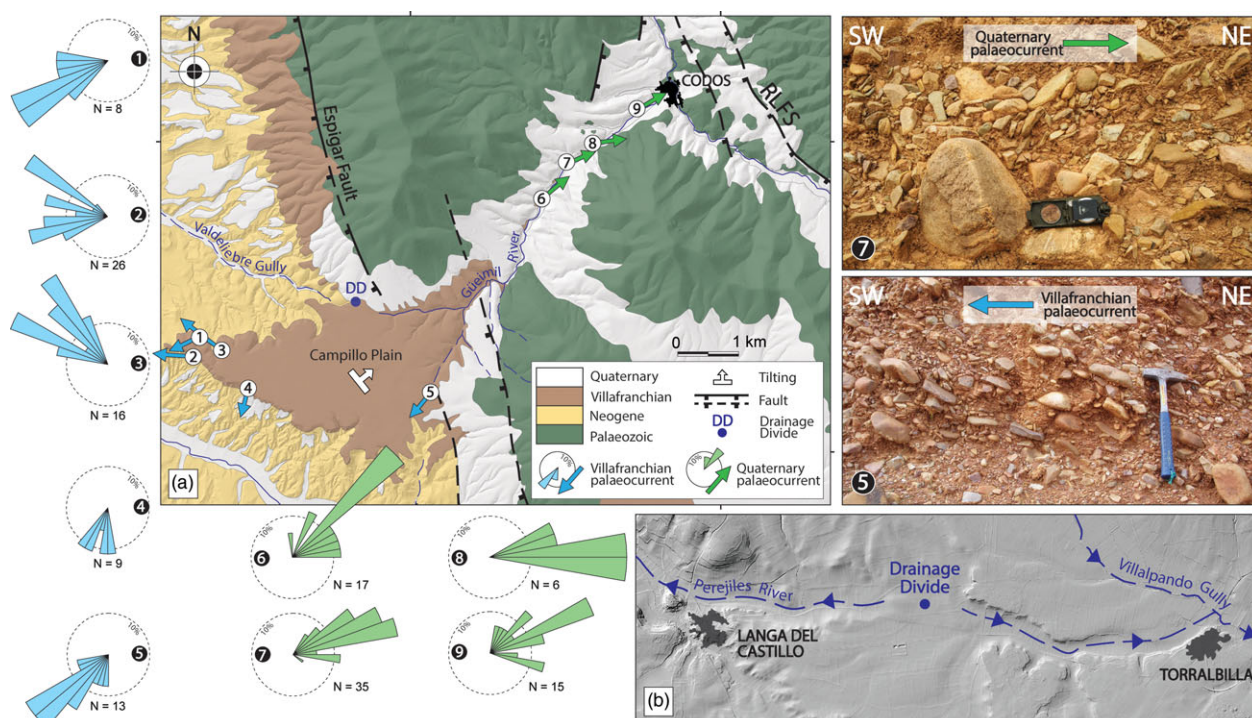


Fig. 6. (Colour online) (a) Drainage reversal at the Güemil valley as indicated by opposite palaeocurrents recorded in Villafranchian and Quaternary deposits (see location in Fig. 5). Blue and green rose diagrams: palaeocurrent distributions inferred from imbricated pebbles measured at sites 1–5 (Villafranchian alluvial system; Pliocene–Pleistocene transition) and sites 5–9 (Quaternary fluvial deposits), respectively. Field views of sites 7 and 9 illustrate the opposite palaeocurrents. (b) Drainage divide of the Perejiles River between Langa del Castillo and Torralbilla (see location in Fig. 5).

fan drainage pattern, and (2) palaeocurrents towards the ENE in Pleistocene fluvial gravel, consistent with the Güemil drainage. The hypothesis is therefore corroborated: the Güemil valley, which in its normal way should drain towards the Perejiles river, was tilted back and then forced to drain into the Grío river, along the same riverbed but flowing in the opposite direction. The anomalous thickness of Pleistocene deposits in the Codos–Tobed sector can be interpreted as a consequence of the increase in accommodation space and subsequent river aggradation also produced by slip on the RLFS.

The regional drainage layout suggests that tilting of the hanging wall of the RLFS has induced other significant anomalies. Tributaries of the Jalón river, namely the Jiloca, the Perejiles and Grío rivers, flow towards the NW or NNW, parallel to recent extensional faults such as the RLFS (Fig. 1c). The high plain of the Calatayud Basin (specifically, the area south of Torralbilla and Mainar) should constitute the natural head of the Perejiles river. Nevertheless, this area drains into the Huerva river (see SE corner of Fig. 5). The continuous, E–W-trending flat-bottomed valley that extends between Torralbilla and Langa del Castillo surprisingly shows divergent drainage. Both the uppermost segment of the W-wards draining Perejiles river, and a short E-wards tributary of the Villalpando gully (flowing into the Huerva river), coexist within that valley. The subtle drainage divide is located on its flat bottom at the halfway point between Torralbilla and Langa del Castillo (Figs 5, 6b). This hydrographic anomaly can also be interpreted as a case of drainage reversal induced by tilting. This would be more recent in age than that interpreted for the Güemil valley, since it occurred within a valley excavated during Pleistocene time. This evidence is consistent with the notion by Gutiérrez *et al.* (2008) of the capture of the Calatayud Basin by the Huerva river during late Pleistocene time.

5.c. Outcrop-scale structural observations

Beyond the geomorphological indicators of tectonic activity, the occurrence of Pleistocene slip on the RLFS should be confirmed by outcrop observations. One of the scarce exposures of the extensional rupture is located SE of Codos (Fig. 7a, b). In this sector, the main fault is accompanied by a smaller antithetic fault, both affecting Palaeozoic and Pleistocene units. Ancient Pleistocene deposits (Pleistocene 1 in Fig. 7a) consist of red conglomerate with sub-angular clasts and occasional silt layers. The Pleistocene 2 unit includes light-brown conglomerate, comprising Palaeozoic angular pebbles, with scarce silt layers. Two samples collected in Pleistocene 1 and 2 units have rendered OSL ages of 66.6 ± 6.5 ka and 40.2 ± 4.4 ka, respectively (see Table 1; location in Fig. 7). Pleistocene 1 is offset by both faults, while Pleistocene 2 deposits fill the intermediate graben (Fig. 7a–c) and could be considered as overall coeval with fault movement. The antithetic fault can be interpreted as a result of secondary accommodation of the hanging-wall block to slip on a curved upper segment of the main fault. The true throw measured at the base of the Pleistocene 1 unit (i.e. the significant vertical displacement, discounting the contribution of the antithetic fault; McCalpin, 1996) is therefore c. 20 m (Fig. 7c).

The RLFS is expressed in this outcrop as a 1–1.5-m-thick fault zone oriented $150, 67^\circ\text{W}$ on average (Fig. 7b), in which Palaeozoic rocks are strongly deformed and partially brecciated. Their Variscan foliation is affected by small-scale drag folds (Fig. 7b'), whose axes are nearly orthogonal to striations observed on discrete rupture surfaces (Fig. 7b''). A nearly pure normal slip, with average transport direction towards 235° , is inferred from such kinematic indicators. Similarly oriented slickenlines have been measured in another outcrop located to the SE (Fig. 7d, d'; see location in

Table 1. Parameters and results of OSL dating of samples collected at the outcrop surveyed SE of Codos (Luminiscence Dating Laboratory of Centro Nacional de Investigación sobre la Evolución Humana, CENIEH, Burgos, Spain; Unit of Radioisotopes, Universidad de Sevilla, Spain)

Sample	Laboratory reference	Stratigraphic location	Depth (m)	H ₂ O (%)	Quartz grain (μm)	²³⁸ U (Bq kg ⁻¹)	²³² Th (Bq kg ⁻¹)	⁴⁰ K (Bq kg ⁻¹)	Dose rate (Gy ka ⁻¹)	Equivalent dose (Gy)	Age (ka)
CODOS_PLE-1	LM20132-08	Pleistocene 1	3	12	180–250	53 ± 27	63 ± 6	0.6 ± 0.1	4.1 ± 0.4	270.9 ± 8.9	66.6 ± 6.5
CODOS_PLE-2	LM20132-09	Pleistocene 2	20	10	180–250	40 ± 23	40 ± 23	0.2 ± 0.1	3.3 ± 0.3	132.8 ± 6.8	40.2 ± 4.4

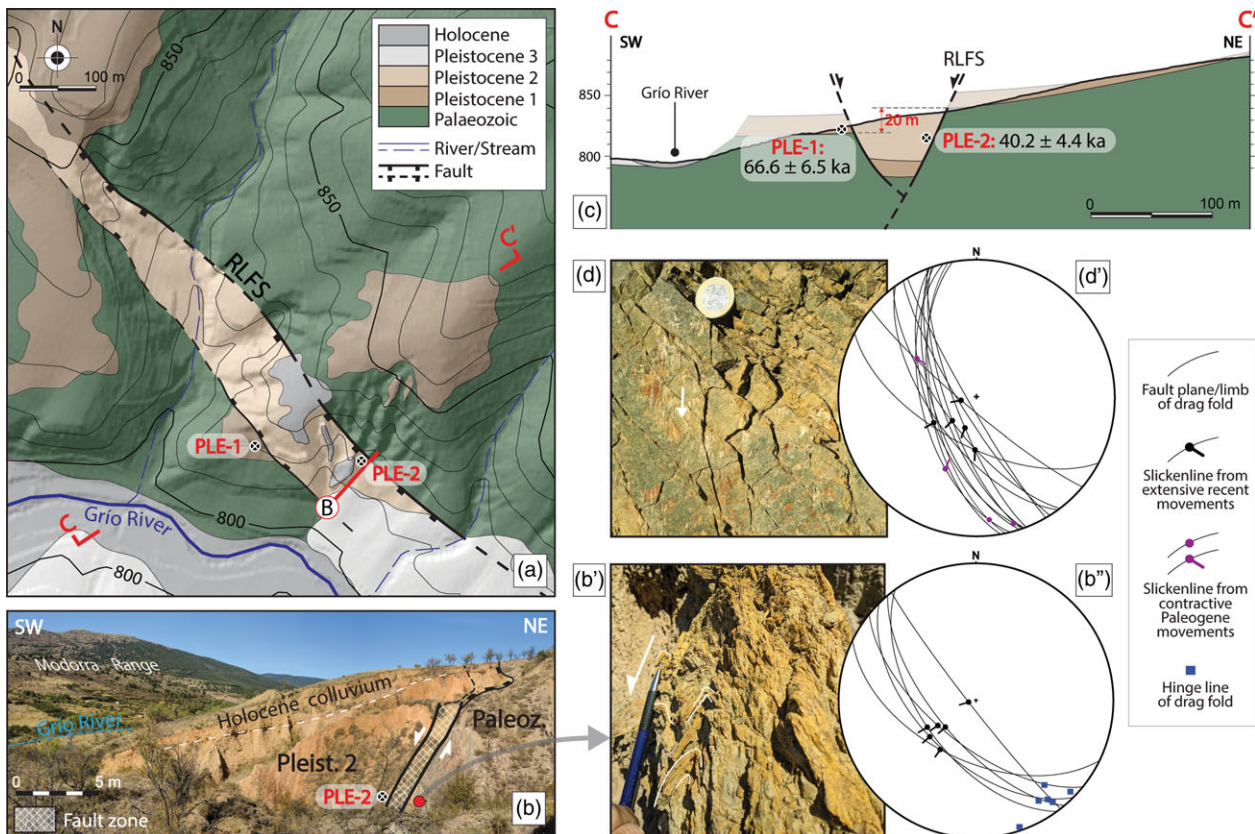


Fig. 7. (Colour online) (a) Geological map of the area SE of Codos showing evidence of Quaternary extensional activity on the Río Grío–Lanzuela Fault Segment (RLFS; see location in Fig. 5). (b) Exposure of the RLFS rupture affecting Quaternary and Palaeozoic units. (b', b'') Field view and orientation of the Variscan foliation affected by Quaternary small-scale drag folds. (c) Cross-section showing vertical displacement of the Pleistocene pediment discounting the contribution of the antithetic fault. (d, d'') Secondary fault planes and slickenlines measured in an outcrop to the SE of map in (a) (see location in Fig. 5). Stereoplots: equal-area, lower hemisphere. The location and age of samples dated by OSL (PLE-1 and PLE-2) is indicated.

Fig. 5). In this second site, extensional slickenlines with accretion quartz fibres overprint previous reverse and strike-slip striations linked to contractive Alpine phases (Fig. 7d).

6. Interpretation and discussion

6.a. Assessing recent activity at the Río Grío–Pancrudo Fault zone

The fracture pattern described in previous sections defines a large recent extensional, NNW–SSE-trending structure, overall oblique to the Calatayud Basin: the Río Grío–Pancrudo Fault Zone, comprising two segments (Río Grío–Lanzuela, RLFS, and Cucalón–Pancrudo, CPFS; Fig. 1c). The maximum vertical offset calculated for the last 3.5 Ma has been identified within the CPFS (Cucalón–Olalla area; Fig. 4a), with a net slip of 325 m and slip rate of 0.09 mm a⁻¹.

Nevertheless, the most conspicuous geomorphological and structural evidence of recent, pure normal slip is found in the RLFS, which should be discussed in detail.

The FES3 planation surface has been used as a mixed, morpho-sedimentary marker for reconstructing the overall morphostructure of the area (Fig. 3). Its age is primarily constrained by robust biostratigraphic and magnetostratigraphic data in the coeval sedimentary units of the Teruel Basin, and secondarily correlated with similar units of the Calatayud Basin (Section 4.d). In this way, its map expression and its age are anchored in both basins at the northern and southern extremes of the study region. We are aware that the contour map of Figure 3 does not directly represent the geometry of tectonic deformation, since height variations of FES2 and FES3 are also partially controlled by their original, not completely flat topography. Nevertheless, the observed regional trends are palaeo-topographically and structurally consistent, and they allow the original slopes (e.g. at the FES3 pediment south

of Pelarda Range) and tectonic tilting (e.g. at the hanging-wall block of the Río Grío–Lanzuela Fault Segment) to be easily distinguished.

By using FES3 as a geomorphological, regionally dated marker (Ezquerro *et al.* 2020), a vertical displacement of *c.* 240 m can be inferred for the last 3.5 Ma in the Codos area (central sector of the RLFS; Fig. 5). Considering an average dip of 67°W and a pure normal slip, this involves a total net slip of *c.* 260 m, and a slip rate of 0.07 mm a⁻¹.

There is also evidence of persistent activity in RLFS during late Pliocene and Pleistocene time, although in this case slip values and slip rates are more uncertain. First, the post-FES4 slip rate cannot be estimated since the age of this marker remains unknown.

Second, a reasonable estimation of the Quaternary slip on RLFS can be made on the basis of roll-over deformation of the Villafranchian pediment, at the Campillo embayment. By extrapolating its tilted surface as far as the main fault trace, and comparing this present-day reconstructed profile with its hypothetical original profile, a minimum throw value has been calculated (Fig. 8a, b). The original slope of the Campillo pediment can be approached using other Villafranchian pediments of the surrounding region as a reference. We have selected 47 pediment remains mapped on the official 1:50 000 National Geological Map (Aragonés *et al.* 1981; del Olmo *et al.* 1983a, b; Hernández *et al.* 1983, 2005; Olivé *et al.* 1983, 2002; Gabaldón *et al.* 1989b) that have not undergone visible deformation. For each of them, the total length and the average slope have been measured and plotted on Figure 8c (see online Supplementary Table S1, available at <http://journals.cambridge.org/geo>). A significant correlation can be recognized between the variables, and a value in the range of 0.5–1° can be inferred as the typical slope of Villafranchian pediments longer than 4 km (which is the case for the Campillo pediment). Using this slope value, the hypothetical original profile of the Villafranchian pediment has been restored in Figure 8a, b, starting from the most distal visible point of the pediment surface (such a procedure implicitly assumes that this point coincides with the rotation axis of roll-over tilting). The difference in height between the original and the present-day profile close to RLFS provides an estimated post-Villafranchian minimum fault throw in the range of 140–220 m, and hence a minimum net slip of 155–235 m. Assuming that the tilted pediment is coeval to the Villafranchian pediments of the Teruel area (*c.* 2.0 Ma; average magnetostratigraphic age of La Puebla de Valverde, see Section 3), the minimum slip rate could be estimated in the range of 0.07–0.11 mm a⁻¹.

The maximum value above inferred for the fault throw (220 m) is close to that obtained from offset of FES3 (240 m), which supports the notion that almost the entire slip recorded at RLFS has occurred after the Villafranchian pediment was modelled. On the contrary, the Espigar fault moved during previous Neogene times and had become inactive by the Pliocene–Pleistocene transition. It generated the mountain front from which the Villafranchian alluvial system was sourced, but no surficial rupture subsequently propagated across the Campillo embayment. In summary, the extensional activity at the NE margin of the Calatayud Basin was transferred from the Espigar fault to the RLFS by early Pleistocene times, as the evolutionary model of Figure 9 illustrates. Both faults, together with local isostatic readjustment (shoulder uplift) at the footwall block of the Daroca fault, were responsible for the overall tilting of the Calatayud Basin. According to Jackson & McKenzie (1983) and Jackson *et al.* (1988), the elevation of the footwall could represent about 10% of the subsidence of the hanging wall with respect to a regional reference level.

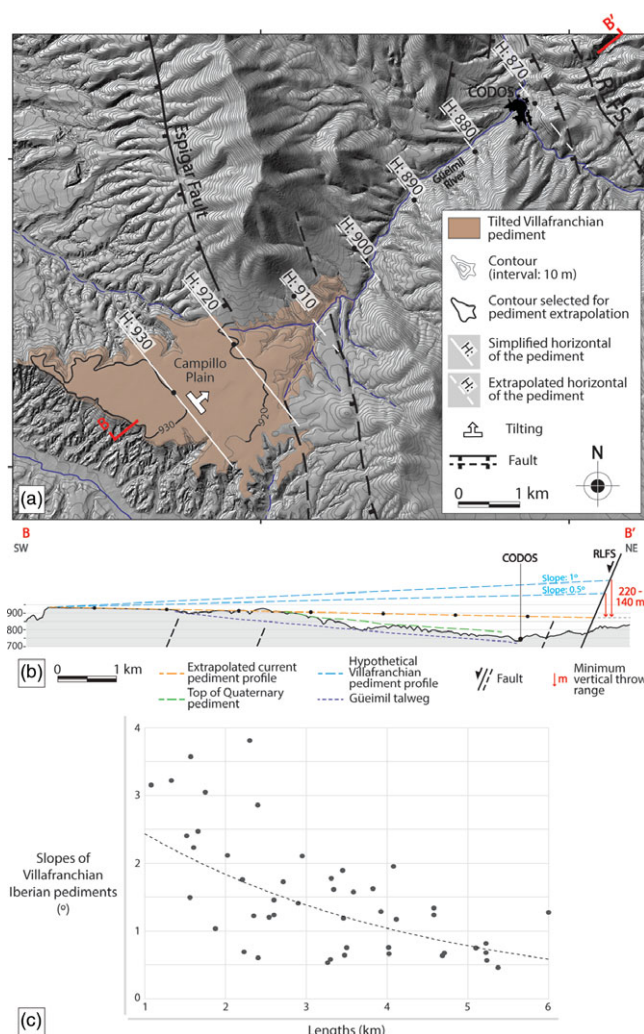


Fig. 8. (Colour online) (a) Extrapolation of the tilted Villafranchian pediment from the Campillo embayment as far as the main trace of the Río Grío–Lanzuela Fault Segment (RLFS; see location in Fig. 5). (b) Extrapolated profile and estimation of the RLFS minimum post-Villafranchian net slip. Topographic heights are expressed in metres above sea level. (c) Relationship between the total length (km) and the slope (°) of the Villafranchian Iberian pediments (see database in online Supplementary Table S1). The trend line (dotted) allows the slope of pediments longer than 4 km to be constrained within the range 0.5–1°.

Finally, concerning the intra-Pleistocene displacement recorded SE of Codos, a throw of 20 m (Fig. 7c) was measured at the base of the Pleistocene 1 unit. The OSL age provided by this unit (66.6 ± 6.5 ka) represents a close supradate of that sedimentary marker (the dated sample was extracted only 4 m above the base). Considering the dip of the fault plane (67°) and the nearly pure normal slip direction, a net slip of *c.* 21.7 m is calculated. A slip rate approaching 0.30–0.36 mm a⁻¹ is therefore inferred for this time period.

6.b. Drainage reversals in the extensional tectonic setting

Sustained activity on the RLFS has produced noteworthy changes in local drainage paths, as well as other sedimentary effects.

- (1) *Drainage reversal along the Güeimil valley (early? Pleistocene).* This flowed towards the SW during the Pliocene–Pleistocene transition (Villafranchian time), feeding a recognizable alluvial

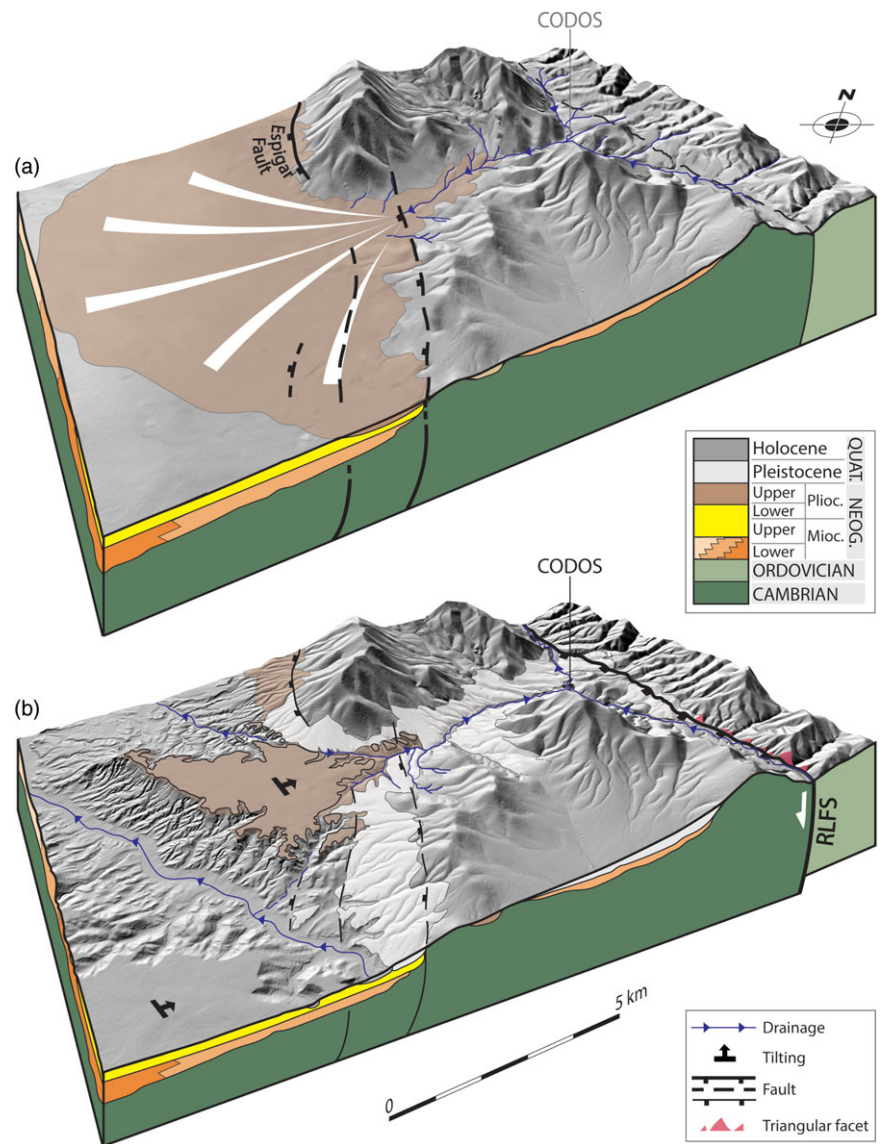


Fig. 9. (Colour online) (a, b) Proposed evolutionary model for the original Codos area, showing successive activation of the Espigar and Río Gúeimil-Lanzuela (RLFS) faults and subsequent drainage reversal along the Güeimil valley. The latter occurred after the Pliocene–Pleistocene transition due to roll-over tilting of the hanging-wall block of the RLFS (see location in Fig. 5). The drainage pattern in the Codos area in (a) is hypothetical.

system in the Calatayud Basin (Fig. 5). Apart from tilting the Neogene units and the FES3 planation surface, roll-over accommodation of the hanging wall of the RLFS switched the slope of the riverbed and forced the Güeimil river to drain towards the NE into the Gúeo river. Migration of the alluvial apex towards the source area during late Neogene time, as well as aggradation of the Güeimil and Gúeo valleys during Pleistocene time, could also result from progressive tilting and consequent increase in accommodation space towards the NE. The block diagrams in Figure 9 illustrate the proposed evolutionary model. In order to estimate the hypothetical extent of the Güeimil palaeo-catchment area illustrated in Figure 9, the relationship between the size of the alluvial fan and its catchment area can be taken into account. According to Dade & Verdeyen (2007), a 15–20 km² alluvial fan (similar to the hypothetical original Campillo) would be associated with a catchment area of c. 35 km². If the palaeo-divide was further from Codos (see Figs 5, 9), the catchment area would attain about 50 km², while with a hypothetical palaeo-divide west of Codos (i.e. originally disconnected Gúeo and Güeimil basins) would be 20–25 km² in size. This means that the location of

this palaeo-divide had probably gone beyond Codos village, although it is not certain that the catchment area was exactly that represented in Figure 9.

- (2) *Drainage reversal along the high Perejiles valley (late Pleistocene).* The natural head of the Perejiles river was captured by the Huerva river, so that a segment of its original, W-wards-draining flat-bottomed valley (between Torralbilla and Langa del Castillo) became a tributary of the Huerva river (Figs 5, 6b).

Examples of drainage reversal were described by Ollier (1981, p. 175–6) west of Lake Victoria (Uganda), induced by tectonic tilting linked to the formation of the Western Rift Valley. Along the SE-flowing Clarence river (eastern Australia), Haworth & Ollier (1992) described evidence of aligned streams that represent the remains of an earlier NW-flowing system, reversed after the tectonic opening of the Tasman Sea. River reversals are also caused by isostatic arching triggered by active tectonics (e.g. opening of the Dead Sea Transform and Rift Valley; Matmon *et al.* 1999). All these examples represent regional-scale drainage anomalies caused by tilting and subsequent migration of drainage divides on footwall blocks of normal faults.

A drainage reversal very similar to that studied in this paper is found in the Megara Basin (central Greece), whose infill currently shows tilting towards the south and is enclosed between ENE–WSW- and WNW–ESE-striking normal faults. The present-day drainage pattern flows S-wards, but sedimentological and drainage analyses reveal that it is the result of a drainage reversal that occurred during late Pleistocene time due to tectonic uplift and tilting (Leeder *et al.* 1991). During the Plio-Pleistocene transition, alluvial clastics from the basin infill were deposited by a NW-flowing system, also corroborated by local palaeocurrents (Bentham *et al.* 1991).

As highlighted in Section 3, the drainage rearrangement of this area of the eastern Iberian Chain took place during a progressive transition from endorheic to exorheic conditions. The overall process is controlled in the distance by base-level changes, in this case of the Ebro river, although it is locally modelled in certain sectors by the activity of nearby faults. The individual influence of each of these factors can be difficult to determine. In our study case, the regional base-level drop would have resulted in divide retreat of the Huerva head, while local NE-tilting of the Calatayud Basin would have contributed to the final drainage reversal.

6.c. Slip rates and seismogenic potential of the Río Grío–Pancrudo Fault Zone within the Iberian Chain context

Slip rates inferred at the Río Grío–Pancrudo Fault Zone for the overall late Pliocene – Quaternary period are close to those reported for the main extensional faults in the eastern Iberian Chain. Since late Pliocene time, faults in both the neighbouring Jiloca graben (Calamocha, Sierra Palomera and Conclud faults) and the Teruel Basin show slip rates within the range of 0.05–0.16 mm a⁻¹ (Simón *et al.* 2012, 2013; Ezquerro *et al.* 2020). These authors noticed that fault slip rates in both basins tend to increase with time (e.g. the slip rate calculated from detailed palaeo-seismological analysis in the Conclud fault for late Pleistocene time is 0.29 mm a⁻¹; Simón *et al.* 2016). The same tendency has been inferred for the Río Grío–Lanzuela Fault Segment studied here: while the average net slip since 3.5 Ma was 0.07 mm a⁻¹, it has increased to a minimum of 0.07–0.11 mm a⁻¹ since 2.0 Ma and has been approaching 0.30–0.36 mm a⁻¹ for the last 66.6 ± 6.5 ka. On the contrary, slip rates on faults closer to the Valencia Trough, such as those of the Maestrat grabens (easternmost Iberian Chain; Simón *et al.* 2012, 2013) and the Catalanian grabens (Masana, 1995; Masana *et al.* 2001; Perea *et al.* 2006), have tended to decrease.

Such a pattern of evolution during Pleistocene time has been associated (Simón *et al.* 2012, 2013; Ezquerro *et al.* 2020) with a number of tectonic processes: (1) progressive W-wards propagation of rifting, from inner parts of the Valencia Trough towards more external domains, as suggested by Capote *et al.* (2002) from the evolutionary trend along Neogene times; (2) favourable orientation of the main Variscan and late Variscan faults that control the macrostructure of the Iberian Chain (NW–SE to NNW–SSE) within the most recent stress field (with dominant extension σ_3 axis trending WSW–ENE; Arlegui *et al.* 2005); (3) fault linkage processes, well documented from tectono-sedimentary analysis in the case of the northern Teruel Basin (Ezquerro, 2017; Ezquerro *et al.* 2019), and also supported by analysis of T-D curves (Ezquerro *et al.* 2020); and (4) (chiefly as a consequence of (2) and (3)), progressive localization of displacement into a few

faults, a tendency that has been observed for example in the central Apennines, Italy, since 0.9 Ma (Roberts *et al.* 2002).

There is evidence of Quaternary activity at the Río Grío–Pancrudo Fault Zone, with decametre-scale displacement at a significant slip rate (close to 0.30–0.36 mm a⁻¹) during late Pleistocene time, allowing us to consider it as an active structure. Its seismogenic potential should therefore be taken into account in the evaluation of seismic hazard of the Iberian Chain. The probability of a single deep fault entirely moving is significant, since the relay zone between the fault segments may not have enough width to act as a barrier to the co-seismic propagation of the surficial rupture. According to Biasi & Wesnousky (2016), ruptures in dip-slip faults manage to cross 54% of relay zones 1 km wide or less, and this percentage increases in the case of normal faults. If we consider the Río Grío–Pancrudo Fault Zone as a single structure, it would generate earthquakes of magnitude 7.3–7.4 (considering a total length of 88 km, and following the correlation of Wells & Coppersmith, 1994). Future detailed palaeo-seismological studies should be focused on assessing the probability of such a scenario.

7. Conclusions

The Río Grío–Pancrudo Fault Zone represents a late Variscan strike-slip structure, reactivated under the Alpine compression during Palaeogene time, and finally inverted during the Neogene–Quaternary extension. It comprises two NNW–SSE-trending fault segments that total about 88 km in length, separated by a right-relay zone 2 km in width and overlapping less than 2 km: Río Grío–Lanzuela (RLFS) and Cucalón–Pancrudo (CPFS). The Río Grío–Pancrudo Fault Zone partially coincides with the northeastern boundary of the Neogene Calatayud Basin, leading to the sinking and overall tilting of its infill (probably with a small contribution of isostatic readjustment at the Daroca fault). Nevertheless, the general trend of the Río Grío–Pancrudo Fault Zone is oblique to the basin boundary: the northern sector of RLFS enters the Palaeozoic Calatayud–Montalbán massif, and the central sector of the CPFS obliquely crosses the basin. Propagation of such a large NNW–SSE-trending extensional structure was possible because of its favourable orientation with respect to the prevailing WSW–ENE σ_3 trajectories of the coeval stress field.

The recent extensional activity of the Río Grío–Lanzuela Fault Segment has been demonstrated and evaluated through its imprint on landforms and drainage. In the Codos area, morphotectonic and palaeocurrent analysis indicate that the Güemil valley has experienced a drainage reversal from flowing into the Calatayud Basin through a wide alluvial fan during Villafranchian time (Pliocene–Pleistocene transition), to flowing into the Grío river following the Río Grío–Lanzuela fault trace after Pleistocene time. The total throw at this sector of the Río Grío–Lanzuela Fault Segment has been calculated at c. 240 m (pure normal net slip of c. 260 m) from offset of an upper Neogene planation surface (FES3; 3.5 Ma), resulting in a long-term slip rate of 0.07 mm a⁻¹. Within the Quaternary, the minimum fault throw is estimated in the range of 140–220 m (pure normal net slip in the range of 155–235 m) for the last 2.0 Ma (slip rate, 0.07–0.11 mm a⁻¹).

Data are more scarce at the Cucalón–Pancrudo Fault Segment, but preliminary results indicate that FES3 has undergone vertical offset of c. 300 m (pure normal net slip, c. 325 m), which implies a slip rate of c. 0.09 mm a⁻¹.

Slip rates obtained in both fault segments are comparable to those averaged on other faults in the central Iberian Chain for late

Pliocene – Pleistocene time. Decametre-scale displacement during late Pleistocene time, at slip rates close to 0.30–0.36 mm a⁻¹, suggests that the fault has undergone an increase in slip rate during Pliocene–Quaternary times, a tendency also previously reported for other faults in the neighbouring Jiloca and Teruel basins.

The seismogenic potential of the Río Grío–Pancrudo Fault Zone, which might be one of the largest active macrostructures in the Iberian Chain, should be considered in the evaluation of seismic hazard of the region. The probability that the coseismic rupture within this fault zone could manage to cross the relay zone between both fault segments, generating earthquakes of magnitude 7.3–7.4, should not be neglected.

Supplementary material. To view supplementary material for this article, please visit <https://doi.org/10.1017/S0016756821000790>

Acknowledgements. This research was financed by Programa Operativo del Fondo Europeo de Desarrollo Regional Aragón 2014–2020 (project LMP127_18) and Ministerio de Ciencia e Innovación of the Spanish Government (project PID2019-108705-GB-I00). This work is a contribution by the Geotransfer-IUCA research group (E32_17R) funded by Aragon Government and FEDER-Aragón 2014–2020 ('Construyendo Europa desde Aragón'). A Peiro benefitted from an FPU contract (FPU17/02470) of the Spanish Government. We thank Alicia Medialdea, as well as the Luminiscence Dating Laboratory of CENIEH (Centro Nacional de Investigación sobre la Evolución Humana, Burgos, Spain) and the Unit of Radioisotopes at the Universidad de Sevilla, for the OSL dating. CL Liesa, LE Arlegui and A Luzón contributed to field survey and interpretation on which the cross-section of Figure 4a is based. MA Soriano helped us with mapping Quaternary pediments in Figure 5. L Ezquerro, L Alcalá and MD Pesquero advised us on issues related to palaeontological dating of planation surfaces and Villafranchian pediments. Finally, we sincerely thank the two anonymous reviewers for their comments and suggestions, which have greatly improved the paper.

Declaration of interest. The authors declare that they have no known competing financial interests or personal relationships that influenced the work reported in this paper.

References

- Adrover R (1975) Principales yacimientos paleomastológicos de la provincia de Teruel y su posición estratigráfica relativa. In *Actas I Coloquio Internacional sobre Bioestratigrafía Continental del Neógeno Superior-Cuaternario Inferior* (eds MT Alberdi and E Aguirre), pp. 31–48. Madrid-Montpellier: Trabajos sobre Neógeno-Cuaternario.
- Adrover R, Feist M, Hugueney M, Mein P and Moissenet E (1982) L'âge et la mise en relief de la formation detritique culminante de la Sierra Pelarda (Prov. Teruel, Espagne). *Comptes rendus de l'Académie des sciences, Paris* **295**, 231–6.
- Allmendinger RW, Cardozo NC and Fisher D (2012) *Structural Geology Algorithms: Vectors & Tensors*. Cambridge: Cambridge University Press, 289 p.
- Álvarez M, Capote R and Vegas R (1979) Un modelo de evolución geotectónica para la Cadena Celtibérica. *Acta Geologica Hispánica* **14**, 172–7.
- Anadón P, Alcalá L, Alonso-Zarza AM, Calvo JP, Ortí F, Rosell L and Sanz-Rubio E (2004) Cuencas de la Cordillera Ibérica. In *Geología de España* (ed JA Vera), pp. 562–69. Madrid: Sociedad Geológica de España-Instituto Geológico y Minero de España.
- Aragonés E, Hernández A, Aguilar MJ, Ramírez J, García-Alcalde GL and Arbizu M (1981) Mapa Geológico de España 1: 50.000, hoja no. 409 (Calatayud). Madrid: Instituto Geológico y Minero de España.
- Arlegui LE, Simón JL, Lisle RJ and Orife T (2005) Late Pliocene–Pleistocene stress field in the Teruel and Jiloca grabens (eastern Spain): contribution of a new method of stress inversion. *Journal of Structural Geology* **27**, 693–705.
- Bentham P, Collier RE, Gawthorpe RL, Leeder R and Stark C (1991) Tectono-sedimentary development of an extensional basin: the Neogene Megara Basin, Greece. *Journal of the Geological Society* **148**, 923–34.
- Biasi GP and Wesnousky SG (2016) Steps and gaps in ground ruptures: empirical bounds on rupture propagation. *Bulletin of the Seismological Society of America* **106**, 1110–24.
- Bonow JM, Lidmar-Bergström K and Japsen P (2006) Palaeosurfaces in central West Greenland as reference for identification of tectonic movements and estimation of erosion. *Global and Planetary Change* **50**, 161–83.
- Burbank DW and Anderson RS (2012) *Tectonic Geomorphology*. Oxford: Wiley-Blackwell, 454 p.
- Calvín-Ballester P and Casas A (2014) Folded Variscan thrusts in the Herrera unit of the Iberian Range (NE Spain). In *Deformation Structures and Processes within the Continental Crust* (eds S Llana-Fúnez, A Marcos and F Bastida), pp. 39–52. Geological Society of London, Special Publication no. 394.
- Campos S, Aurell M and Casas A (1996) Origen de las brechas de la base del Jurásico en Morata de Jalón. *Geogaceta* **20**, 887–9.
- Capote R, Muñoz JA, Simón JL, Liesa CL and Arlegui LE (2002) Alpine tectonics I: The Alpine system north of the Betic Cordillera. In *Geology of Spain* (eds W Gibbons and T Moreno), pp. 367–400. Geological Society of London.
- Cardozo N and Allmendinger RW (2013) Spherical projections with OSXStereonet. *Computers & Geosciences* **51**, 193–205.
- Casas A, Aurell M, Revuelto C, Calvín P, Simón JL, Pueyo Ó, Pocoví A and Marcén M (2017) El embalse de Mularroya (Zaragoza): problemas geológicos de una obra en estado avanzado de construcción. *Revista de la Sociedad Geológica de España* **30**, 51–64.
- Casas A, Marcén M, Calvín P, Gil A, Román-Berdiel T and Pocoví A (2016) Deformación varisca, tardivarisca y alpina en la Rama Aragonesa de la Cordillera Ibérica: propuesta para diferenciación y denominación de estructuras. *Geo-Temas* **16**, 495–8.
- Colomer M and Santanach P (1988) Estructura y evolución del borde sur-occidental de la Fosa de Calatayud-Daroca. *Geogaceta* **4**, 29–31.
- Cortés-Gracia AL and Casas-Sáinz A (1996) Deformación alpina de zócalo y cobertera en el borde norte de la Cordillera Ibérica (Cubeta de Azuara-Sierra de Herrera). *Revista de la Sociedad Geológica de España* **9**, 51–66.
- Dade WB and Verdeyen ME (2007) Tectonic and climatic controls of alluvial-fan size and source-catchment relief. *Journal of the Geological Society*, **164**, 353–8.
- de Vicente G, Vegas R, Muñoz-Martín A, Wees JDVan, Casas-Sáinz A, Sopena A, Sánchez-Moya Y, Arche A, López-Gómez J, Olaiz A and Fernández-Lozano J (2009) Oblique strain partitioning and transpression on an inverted rift: The Castilian Branch of the Iberian Chain. *Tectonophysics* **470**, 224–42.
- del Olmo P, Hernández A, Aragonés E, Gutiérrez M, Puigdefábregas C, Giner J, Aguilar MJ, Leal MC, Gutiérrez JC, Gil M, Adrover R, Portero JM and Gabaldón V (1983a) Mapa Geológico de España 1: 50.000, hoja no. 437 (Ateca). Madrid: Instituto Geológico y Minero de España.
- del Olmo P, Portero JM, Villena J, Pardo G, Gutiérrez M, Puigdefábregas C, Giner J, Aguilar MJ, Leal MC, Goy A, Comas MJ and Gabaldón V (1983b) Mapa Geológico de España 1: 50.000, hoja no. 490 (Odón). Madrid: Instituto Geológico y Minero de España.
- Ezquerro L (2017) El sector norte de la cuenca neógena de Teruel: tectónica, clima y sedimentación. Ph.D. thesis, Universidad de Zaragoza. Published thesis.
- Ezquerro L, Lafuente P, Pesquero MD, Alcalá L, Arlegui LE, Liesa CL, Luque L, Rodríguez-Pascua MA and Simón JL (2012) Una cubeta endorreica residual Plio-Pleistocena en la zona de relevo entre las fallas de Concud y Teruel: implicaciones paleogeográficas. *Revista de la Sociedad Geológica de España* **25**, 157–75.
- Ezquerro L, Luzón A, Liesa CL and Simón JL (2019) Alluvial sedimentation and tectono-stratigraphic evolution in a narrow extensional zigzag basin margin (northern Teruel Basin, Spain). *Journal of Palaeogeography* **8**, 1–25.
- Ezquerro L, Simón JL, Luzón A and Liesa CL (2020) Segmentation and increasing activity in the Neogene–Quaternary Teruel Basin rift (Spain) revealed by morphotectonic approach. *Journal of Structural Geology* **135**, published online 26 March 2020. doi: [10.1016/j.jsg.2020.104043](https://doi.org/10.1016/j.jsg.2020.104043)
- Gabaldón V, Lendínez A, Ferreiro E, Ruiz V, López de Alda F, Valverde M, Lago San José M, Meléndez A, Pardo G, Ardevol L, Villena J, González A, Hernández A, Álvarez M, Leal MC, Aguilar Tomás M, Gómez JJ and

- Carls P (1991) Mapa Geológico de España 1: 200.000, hoja no. 40 (Daroca). Madrid: Instituto Geológico y Minero de España.
- Gabaldón V, Lendínez A, Ruiz V, Carls P, Alvaro M, Gutiérrez M, Hernández A, Gómez JJ, Meléndez A, Perez A, Pardo G, Villena J, Aguilar M, Leal MC, Comas MJ, Goy A, Lago M and Conte JC (1989a) Mapa Geológico de España 1: 50.000, hoja no. 466 (Moyuela). Madrid: Instituto Geológico y Minero de España.
- Gabaldón V, Lendínez A, Ruiz V, Carls P, Alvaro M, Gutiérrez M, Soriano MA, Hernández A, Gómez JJ, Meléndez A, Aurell M, Pérez A, Pardo G, Villena J, Aguilar M, Leal MC, Comas MJ, Goy A, Lago M and Conte JC (1989b) Mapa Geológico de España 1: 50.000, hoja no. 439 (Azua). Madrid: Instituto Geológico y Minero de España.
- Goldsworthy M and Jackson J (2000) Active normal fault evolution in Greece revealed by geomorphology and drainage patterns. *Journal of the Geological Society* **157**, 967–81.
- Gracia FJ, Gutiérrez M and Leránoz B (1988) Las superficies de erosión neógenas en el sector central de la Cordillera Ibérica. *Revista de la Sociedad Geológica de España* **1**, 135–42.
- Gracia J (1992) Tectónica pliocena de la Fosa de Daroca (prov. de Zaragoza). *Geogaceta* **11**, 127–9.
- Guimerà J (1988) Estudi estructural de l'enllaç entre la Serralada Ibèrica i la Serralada Costanera Catalana. Ph.D. thesis, Universitat de Barcelona. Published thesis.
- Gutiérrez F, Gracia FJ and Gutiérrez M (1996) Consideraciones sobre el final del relleno endorreico de las fosas de Calatayud y Teruel y su paso al exorreísmo: implicaciones morfoestratigráficas y estructurales. In *IV Reunión de Geomorfología* (eds A Grandal and J Pagés), pp. 23–43. O Castro, A Coruña: Sociedad Española de Geomorfología.
- Gutiérrez F, Gutiérrez M, Gracia FJ, McCalpin JP, Lucha P and Guerrero J (2008) Plio-Quaternary extensional seismotectonics and drainage network development in the central sector of the Iberian Chain (NE Spain). *Geomorphology* **102**, 21–42.
- Gutiérrez F, Lucha P and Jordá L (2013) The Río Grío depression (Iberian Chain, NE Spain). Neotectonic graben vs. Fluvial valley. *Cuaternario y Geomorfología* **27**, 5–32.
- Gutiérrez F, Moreno D, López GI, Jiménez F, del Val M, Alonso MJ, Martínez-Pillado V, Guzmán O, Martínez D and Carbonel D (2020) Revisiting the slip rate of Quaternary faults in the Iberian Chain, NE Spain. Geomorphic and seismic-hazard implications. *Geomorphology*, **363**, 107233.
- Haworth RJ and Ollier CD (1992) Continental rifting and drainage reversal: the Clarence River of eastern Australia. *Earth Surface Processes and Landforms* **17**, 387–97.
- Hernández A, Olivé A, Moissenet E, Pardo G, Villena J, Portero JM, Gutiérrez M, Puigdefábregas C, Giner J, Aguilar MJ, Leal MC, Gutiérrez JC, Gil MD, Adrover R and Gabaldón V (1983) Mapa Geológico de España 1: 50.000, hoja no. 491 (Calamocha). Madrid: Instituto Geológico y Minero de España.
- Hernández A, Ramírez JI, Navarro JJ, Cortes AL, Rodríguez R, Babiano F, Gómez D, Ramírez J, Cuenca G, Pozo M and Casas J (2005) Mapa Geológico de España 1: 50.000, hoja no. 411 (Longares). Madrid: Instituto Geológico y Minero de España.
- Herraiz M, De Vicente G, Lindo-Ñaupari R, Giner J, Simón JL, González-Casado JM, Vadillo O, Rodríguez-Pascua MA, Cicuéndez JL, Casas A, Cabañas L, Rincón P, Cortés AL, Ramírez M and Lucini M (2000) The recent (upper Miocene to Quaternary) and present tectonic stress distributions in the Iberian Peninsula. *Tectonics* **19**, 762–86.
- Jackson J, Norris R and Youngson J (1996) The structural evolution of active fault and fold systems in central Otago, New Zealand: evidence revealed by drainage patterns. *Journal of Structural Geology* **18**, 217–34.
- Jackson JA and McKenzie D (1983) The geometrical evolution of normal fault systems. *Journal of Structural Geology* **5**, 471–82.
- Jackson JA, White NJ, Garfunkel Z and Anderson H (1988) Relations between normal fault geometry, tilting and vertical motions in extensional terrains: an example from the southern Gulf of Suez. *Journal of Structural Geology* **10**, 155–70.
- Julivert M (1954) *Observaciones sobre la tectónica de la Depresión de Calatayud*. Sabadell: Museo de Sabadell, 17 p.
- Keller EA (1986) Investigation of active tectonics: use of surficial earth processes. In *Active Tectonics: Impact on Society* (ed RR Wallace), pp. 136–147. Washington DC: National Academic Press.
- Lafuente P, Arlegui LE, Liesa CL, Pueyo O and Simón JL (2014) Spatial and temporal variation of paleoseismic activity at an intraplate, historically quiescent structure: the Conclud fault (Iberian Chain, Spain). *Tectonophysics* **632**, 167–87.
- Leeder MR and Jackson JA (1993) The interaction between normal faulting and drainage in active extensional basins, with examples from the western United States and central Greece. *Basin Research* **5**, 79–102.
- Leeder MR, Seger MJ and Stark CP (1991) Sedimentation and tectonic geomorphology adjacent to major active and inactive normal faults, southern Greece. *Journal of the Geological Society* **148**, 331–43.
- Liesa CL, Simón JL, Ezquerro L, Arlegui LE and Luzón A (2019) Stress evolution and structural inheritance controlling an intracontinental extensional basin: the central-northern sector of the Neogene Teruel Basin. *Journal of Structural Geology* **118**, 362–76.
- Maillard A and Mauffret A (1999) Crustal structure and riftogenesis of the Valencia Trough (north-western Mediterranean Sea). *Basin Research*, **11**, 357–79.
- Marcén M (2020) Fábricas Magnéticas aplicadas al estudio de Zonas de Falla: Ejemplos de la Península Ibérica. Ph.D. thesis, Universidad de Zaragoza. Published thesis.
- Marcén M and Román-Berdiel MT (2015) Geometría y cinemática de la zona de falla de Río Grío: evidencias de transpresión alpina en la Cadena Ibérica. *Geogaceta* **58**, 180–3.
- Martín M, Canerot J, Linares-Rivas A, Grambast L, Quintero I, Mansilla H, De las Heras A, Fernández MC, Leyva F and Martínez JU (1977) Mapa Geológico de España 1: 50.000, hoja no. 492 (Segura de los Baños). Madrid: Instituto Geológico y Minero de España.
- Martín-Bello L, Arlegui LE, Ezquerro L, Liesa CL and Simón JL (2014) La falla de Calamocha (fosa del Jiloca, Cordillera Ibérica): estructura y actividad pleistocena. In *Una aproximación multidisciplinaria al estudio de las fallas activas, los terremotos y el riesgo sísmico* (eds A Álvarez-Gómez and F Martín-González), pp. 55–58. Lorca, Murcia, 22–24 October 2014. 2ª Reunión Ibérica sobre Fallas Activas y Paleoseismología.
- Masana E (1995) L'activitat neotectònica a les cadenes Costaneres Catalanes. Ph.D. thesis, Universitat de Barcelona. Published thesis.
- Masana E, Villamarín JA and Santanach P (2001) Paleoseismic results from multiple trenching analysis along a silent fault: the El Camp fault (Tarragona, northeastern Iberian Peninsula). *Acta Geologica Hispánica* **36**, 329–54.
- Mateu J (1982) El Norte del País Valenciano. Geomorfología litoral y prelitoral. Ph.D. thesis, Universitat de Valencia. Published thesis.
- Matmon A, Enzel Y, Zilberman E and Heimann A (1999) Late Pliocene and Pleistocene reversal of drainage systems in northern Israel: tectonic implications. *Geomorphology* **28**, 43–59.
- McCalpin JP (1996) *Paleoseismology*. San Diego: Academic Press, 588 p.
- Moissenet É (1980) Relief et déformations récentes: trois transversales dans les fossés internes des chaînes ibériques orientales. *Revue géographique des Pyrénées et du Sud-Ouest, Sud-Ouest Européen* **51**, 315–44.
- Olivé A, del Olmo P, Portero JM, Carls P, Szduy K, Collande CV, Kolb S, Teyssen T, Gutiérrez M, Puigdefábregas C, Giner J, Aguilar MJ, Leal MC, Goy A, Comas MJ, Adrover R and Gabaldón V (1983) Mapa Geológico de España 1: 50.000, hoja no. 438 (Paniza). Madrid: Instituto Geológico y Minero de España.
- Olivé A, Hernández A, Moissenet E, Pardo G, Villena J, Gutiérrez M, Puigdefábregas C, Giner J, Aguilar MJ, Leal MC, Goy A, Comas MJ, Adrover R, Portero JM and Gabaldón V (2002) Mapa Geológico de España 1: 50.000, hoja no. 516 (Monreal del Campo). Madrid: Instituto Geológico y Minero de España.
- Ollier C (1981) *Tectonics and Landforms*. London: Longman, 324 pp.
- Pailhé P (1984) La Chaîne Ibérique Orientale. Étude géomorphologique. Ph.D. thesis, Université de Bordeaux. Published thesis.
- Peña JL, Gutiérrez M, Ibáñez MJ, Lozano MV, Rodríguez J, Sánchez-Fabre M, Simón JL, Soriano MA and Yetano LM (1984) *Geomorfología de la provincia de Teruel*. Teruel: Instituto de Estudios Turolenses, 149 p.

- Perea H, Masana E and Santanach P** (2006) A pragmatic approach to seismic parameters in a region with low seismicity: the case of Eastern Iberia. *Natural Hazards* **39**, 451–77.
- Pérez A, Pardo G, Villena J and González A** (1983) Estratigrafía y sedimentología del Paléogeno de la cubeta de Montalbán, prov. de Teruel, España. *Boletín de la Real Sociedad Española de Historia Natural, Sección Geológica* **81**, 197–223.
- Pérez A and Simón JL** (1993) Cambios en el trazado de la red fluvial producidos por la tectónica cuaternaria en el sistema de fosas del Maestrat. *El Cuaternario de España y Portugal, ITGE-AEQUA, Madrid* **2**, 707–15.
- Roberts GP, Michetti AM, Cowie P, Morewood NC and Papanikolaou I** (2002) Fault slip-rate variations during crustal-scale strain localisation, central Italy. *Geophysical Research Letters* **29**, 9-1.
- Roca E and Guimerá J** (1992) The Neogene structure of the eastern Iberian margin: structural constraints on the crustal evolution of the Valencia trough (western Mediterranean). *Tectonophysics* **203**, 203–18.
- Rubio JC** (2004) *Estudio hidrogeológico e histórico arqueológico de los humedales del alto Jiloca*. Zaragoza: Consejo de Protección de la Naturaleza de Aragón, 216 p.
- Rubio JC and Simón JL** (2007) Tectonic subsidence vs. erosional lowering in a controversial intramontane depression: the Jiloca basin (Iberian Chain, Spain). *Geological Magazine* **144**, 1–15.
- Sanz-Rubio E** (1999) Análisis de los sistemas deposicionales carbonáticos y evaporíticos del Neógeno de la Cuenca de Calatayud (provincia de Zaragoza). Ph.D. thesis, Universidad Complutense de Madrid. Published thesis.
- Sanz-Rubio E, Sánchez-Moral S, Cañaveras JC, Abdul-Aziz H, Calvo JP, Cuezva S, Mazo AV, Rouchy JM, Sesé C and Van Darn J** (2003) Síntesis de la cronoestratigrafía y evolución sedimentaria de los sistemas lacustres evaporíticos y carbonatados neógenos de la cuenca de Calatayud-Montalbán. *Estudios Geológicos* **59**, 83–105.
- Scotti VN, Molin P, Faccenna C, Soligo M and Casas-Sainz A** (2014) The influence of surface and tectonic processes on landscape evolution of the Iberian Chain (Spain): quantitative geomorphological analysis and geochronology. *Geomorphology* **206**, 37–57.
- Simón JL** (1982) Compresión y distensión alpinas en la Cadena Ibérica Oriental. Ph.D. thesis, Universidad de Zaragoza. Published thesis.
- Simón JL** (1989) Late Cenozoic stress field and fracturing in the Iberian Chain and Ebro Basin (Spain). *Journal of Structural Geology* **11**, 285–94.
- Simón JL, Arlegui LE, Ezquerro L, Lafuente P, Liesa CL and Luzón A** (2016) Enhanced palaeoseismic succession at the Concud Fault (Iberian Chain, Spain): new insights for seismic hazard assessment. *Natural Hazards* **80**, 1967–93.
- Simón JL, Arlegui LE, Ezquerro L, Lafuente P, Liesa CL and Luzón A** (2017) Assessing interaction of active extensional faults from structural and paleoseismological analysis: The Teruel and Concud faults (eastern Spain). *Journal of Structural Geology* **103**, 100–19.
- Simón JL, Arlegui L, Lafuente P and Liesa CL** (2012) Active extensional faults in the central-eastern Iberian Chain, Spain. *Journal of Iberian Geology* **38**, 127–44.
- Simón JL, Ezquerro L, Arlegui LE, Liesa CL, Luzón A, Medialdea A, García A and Zarazaga D** (2019) Role of transverse structures in paleoseismicity and drainage rearrangement in rift systems: the case of the Valdecebro fault zone (Teruel graben, eastern Spain). *International Journal of Earth Sciences* **108**, 1429–49.
- Simón JL, Pérez-Cueva AJ and Calvo-Cases A** (2013) Tectonic beheading of fluvial valleys in the Maestrat grabens (eastern Spain): insights into slip rates of Pleistocene extensional faults. *Tectonophysics* **593**, 73–84.
- Simón-Porcari G, Simón JL and Liesa CL** (2019) La cuenca neógena extensional de El Pobo (Teruel, Cordillera Ibérica): sedimentología, estructura y relación con la evolución del relieve. *Revista de la Sociedad Geológica de España* **32**, 17–42.
- Sinusía C, Pueyo EL, Azanza B and Pocoví A** (2004) Datación magnetoestratigráfica del yacimiento paleontológico de La Puebla de Valverde (Teruel). *Geo-Temas* **6**, 339–42.
- Tena S and Casas A** (1996) Estructura y cinemática de la falla de Alpeñés (Cordillera Ibérica). *Geogaceta* **20**, 789–91.
- Vacherat A, Bonnet S and Mouthereau F** (2018) Drainage reorganization and divide migration induced by the excavation of the Ebro basin (NE Spain). *Earth Surface Dynamics* **6**, 369–387.
- Vegas R, Fontboté JM and Banda E** (1979) Widespread Neogene rifting superimposed on alpine regions of the Iberian Peninsula. Proceedings of the Symposium on Evolution and Tectonics of the Western Mediterranean and Surrounding Areas, EGS, Vienna. Madrid: Instituto Geográfico Nacional, Special Publication no. 201, 109–128.
- Wagner T, Fritz H, Stüwe K, Nestroy O, Rodnight H, Hellstrom J and Benischke R** (2011) Correlations of cave levels, stream terraces and planation surfaces along the River Mur: Timing of landscape evolution along the eastern margin of the Alps. *Geomorphology* **134**, 62–78.
- Wells DL and Coppersmith KJ** (1994) New empirical relationships among magnitude, rupture length, rupture width, rupture area and surface displacement. *Bulletin of the Seismological Society of America* **84**, 974–1002.